Experimental Dermatology ADF

Early onset of senescence and imbalanced epidermal homeostasis across the decades in photoexposed human skin: fingerprints of inflammaging.

Journal:	*Experimental Dermatology*
Manuscript ID	EXD-22-0133.R1
Wiley - Manuscript type:	Research Article
Date Submitted by the Author:	11-Jun-2022
Complete List of Authors:	Jarrold, Bradley B.; The Procter & Gamble Company Cincinnati OH USA Tan, Christina Yan Ru; A*STAR Skin Research Labs Singapore Singapore Ho, Chin Yee; A*STAR Skin Research Labs Singapore Singapore Soon, Ai Ling; A*STAR Skin Research Labs Singapore Singapore Lam, TuKiet; Keck MS & Proteomics Resource Yale School of Medicine New Haven CT USA Yang, Xiaojing; Zymo Research Corporation Irvine CA USA Nguyen, Calvin; Zymo Research Corporation Irvine CA USA Guo, Wei; Zymo Research Corporation Irvine CA USA Chew, Yap Ching; Zymo Research Corporation Irvine CA USA DeAngelis, Yvonne; The Procter & Gamble Company Cincinnati OH USA Costello, Lydia; Durham University Durham UK De Los Santos Gomez, Paola; Durham University Durham UK Przyborski, Stefan ; Durham University Durham UK Bellanger, Sophie; A*STAR Skin Research Labs Singapore Singapore Dreesen, Oliver; A*STAR Skin Research Labs Singapore Singapore Kimball, Alexa ; Beth Israel Deaconess Medical Center and Harvard Medical School Boston MA USA Oblong, John; The Procter & Gamble Company Cincinnati OH USA
Area of Expertise:	Skin aging, Keratinocyte biology and epidermal physiology, Photobiology and photodermatology
Additional Keywords:	AGEING, BIOMARKERS, EPIDERMAL DIFFERENTIATION, INFLAMMATION, SENESCENCE
Keywords:	Epidermis, photoexposed, inflammation, inflammaging, epidermal morphology

Early onset of senescence and imbalanced epidermal homeostasis across the decades in photoexposed human skin: fingerprints of inflammaging.

Bradley B. Jarrold[1], Christina Yan Ru Tan[2], Chin Yee Ho[2], Ai Ling Soon[2], TuKiet T. Lam[3], Xiaojing Yang[4], Calvin Nguyen[4], Wei Guo[4], Yap Ching Chew[4], Yvonne M. DeAngelis[1], Lydia Costello[5], Paola De Los Santos Gomez[5], Stefan Przyborski[5], Sophie Bellanger[2], Oliver Dreesen[2], Alexa B. Kimball[6], and John E. Oblong[1]

[1]The Procter & Gamble Company, Cincinnati, OH, USA; [2]A*STAR Skin Research Labs, Singapore, Singapore; [3]Keck MS & Proteomics Resource, Yale School of Medicine, New Haven, CT, USA; [4]Zymo Research Corporation, Irvine, CA, USA; [5]Durham University, Durham, UK; [6]Beth Israel Deaconess Medical Center and Harvard Medical School, Boston, MA, USA

Correspondence: John E. Oblong, The Procter & Gamble Company, Cincinnati, OH, 45040, USA. E-mail: oblong.je@pg.com

Short title: Chronic inflammation remains elevated across decades in a 20's to 70's year old cohort.

Keywords: Epidermis, photoexposed, inflammation, inflammaging, epidermal morphology, senescence, differentiation, glycolysis, hypoxia, and epigenetics

Abbreviation list

LCM: laser capture microdissection

SASP: senescence-associated secretory phenotype

DEJ: dermal epidermal junction

UEA-1: *Ulex Europaeus*-I Lectin

53BP1: p53-binding protein 1

IL-8: interleukin-8

IL-1α: interleukin-1α

IL-1RA: interleukin-1 receptor antagonist

FLG: filaggrin

INV: involucrin

ALOX12B: arachidonate 12-lipoxygenase,12R

LOR: loricrin

KRT2: keratin 2

KRT14: keratin 14

CALML3: calmodulin-like protein 3

SPINK5: serine protease inhibitor Kazai-type 5

CSTB: cystatin B

KLF9: Krüppel-like factor 9

IGF1R: insulin like growth factor 1 receptor

LCE2C: late cornified envelope 2C

CAPN1: calpain 1

CDKN2A: cyclin dependent kinase inhibitor 2A

CRYAB: alpha-crystallin B chain

CXCR2: cytokine receptor type 2/IL8RB

mTOR: mammalian target of rapamycin

RBL2: retinoblastoma-like protein 2

SIRT1: sirtuin 1

HIF1α: hypoxia inducible factor 1, subunit alpha

HBA: hemoglobin-α

HBB: hemoglobin-β

HMOX1: heme oxygenase 1

SLC7A11: cystine/glutamate antiporter

ALDOA: aldolase A

KDM3A: lysine demethylase 3A

KDM5A: lysine demethylase 5A

SPRY2: Sprouty homolog 2

LDHA: lactate dehydrogenase A

PGM1: phosphoglucomutase 1

ABSTRACT

Inflammaging is a theory of aging which purports that low-level chronic inflammation leads to cellular dysfunction and premature aging of surrounding tissue. Skin is susceptible to inflammaging because it is the first line of defense from the environment, particularly solar

radiation. To better understand the impact of aging and photoexposure on epidermal biology, we performed a systems biology-based analysis of photoexposed face and arm, and photoprotected buttock sites, from women between the ages of 20's to 70's. Biopsies were analyzed by histology, transcriptomics, and proteomics and skin surface biomarkers collected from tape strips. We identified morphological changes with age of epidermal thinning, rete ridge pathlength loss, and stratum corneum thickening. The SASP biomarkers IL-8 and IL-1RA/IL1-α were consistently elevated in face across age and *cis/trans*-urocanic acid were elevated in arms and face with age. In older arms, the DNA damage response biomarker 53BP1 showed higher puncti numbers in basal layers and epigenetic aging was accelerated. Genes associated with differentiation and senescence showed increasing expression in the 30's whereas genes associated with hypoxia and glycolysis increased in the 50's. Proteomics comparing 60's vs 20's confirmed elevated levels of differentiation and glycolytic related proteins. Representative immunostaining for proteins of differentiation, senescence, and oxygen sensing/hypoxia showed similar relationships. This systems biology-based analysis provides a body of evidence that young photoexposed skin is undergoing inflammaging. We propose the presence of chronic inflammation in young skin contributes to an imbalance of epidermal homeostasis that leads to a prematurely aged appearance during later life.

1 INTRODUCTION

The skin is one of the largest organs of the human body, providing protection from external insults such as solar radiation, pollution, chemicals, and particulate matter. Like all organs of the body, the skin is susceptible to aging, resulting in structural and

functional changes which may be accelerated further by environmental insults.[1] This premature aging of skin leads to cellular and morphological changes that accumulate over time and ultimately affect the skin's appearance, functionality, and homeostatic state. This homeostasis is dependent on an organized and timely renewal process, initiated by basal keratinocytes which proliferate and differentiate to ultimately transform into corneocytes that comprise the stratum corneum. An imbalance in this process has implications on skin's appearance, health, and response to stress. Thus, it is essential to understand these changes to identify mechanistic intervention targets that would prevent and repair premature aging and maintain skin health and appearance.

We previously reported findings from a large base study that evaluated biopsies collected from photoexposed face and dorsal forearms as well as photoprotected buttock sites of Caucasian females across age decades spanning 20's to the 70's, demonstrating that age impacts a wide range of molecular processes in skin.[2] Given that a low grade chronic inflammatory state is hypothesized to be a significant contributor to premature aging in the inflammaging theory, we asked whether this phenomenon could be observed in our previously reported skin biopsy study and investigated its potential impact on epidermal biology and homeostasis. A systems biology-based analysis of skin surface biomarkers, transcriptomics, proteomics, metabolomics, histology, and immunostaining confirmed that there is underlying chronic inflammation in photoexposed face skin that remains elevated across the decades. Primarily in photoexposed skin, we found an imbalance in epidermal homeostasis beginning in the 20's to 30's and elevation of senescence-related components in the 30's to 40's. A subsequent increase of oxygen sensing/hypoxia and metabolic shift

towards glycolysis occurs in the 50's. Additionally, there is a higher epigenetic aging rate in 60's when comparing to the 30's and is further elevated by photoexposure. Based on these findings, we propose that photoexposed skin undergoes inflammaging which may play a role in the molecular and morphological changes that ultimately lead to a photoaged appearance and less healthy state of skin.

2 MATERIALS AND METHODS

The detailed protocols and statistical analysis are described in Supplemental Materials and Methods.

3 RESULTS

3.1 Age-associated changes in epidermal morphology

We first performed a histomorphometric analysis of the structural compartments of the epidermis from buttock, arm, and face sites across age groups. With age, the overall thickness of the stratum corneum increases (Figure 1A) whereas the epidermal layer becomes thinner (Figure 1B), and the rete ridge path length ratio decreases (Figure 1C). Comparison of the mean data between the 20's and each decade showed that these changes become statistically significant in the older age groups (Supplemental Table 1). A representative histological stain from a 20's and a 60's year old face highlights these structural changes (Figure 1D). In an older age sample, we observed relatively lower detection of microcapillary structures using staining against UEA-1, a lectin that binds to endothelial related cells.[3] A representative image shows the

differential staining pattern below the basement membrane (Figure 1E, white arrows) as well as staining in the stratum granulosum and corneum. This pattern is similar to what has been previously reported in skin.[3] The structural changes of thickening of the stratum corneum and the thinning of the epidermis suggest an imbalance between proliferation and differentiation that changes with age across all body sites.

3.2 Proteomics analysis shows elevated presence of proteins associated with differentiation and glycolysis in 60's aged dorsal forearm epidermis over 20's age group.

To better understand these measured changes in epidermal structure with age, LCM isolated epidermal sections from 20's and 60's dorsal arms were processed and analysed by label free quantitative mass spectrometry. Out of 367 proteins identified, 83 showed a significant difference (p<0.1) in levels when comparing between the two age groups (Supplemental Table 2). Of the 83 proteins, 24 proteins were associated with epidermal differentiation and metabolism/oxygen sensing (Table 1). 23 of these had a similar directional relationship with their representative gene expression pattern with age. The exception is calpain 1 (CAPN1) which showed no significant change in expression levels across the decades (data not shown). Interestingly, we also detected a higher numerical level of hemoglobin-α (p=0.092) and hemoglobin-β (p=0.134, data not shown) present in the older group.

3.3 Imbalance in epidermal differentiation/proliferation increases with age in photoexposed epidermis.

To further understand the age-associated changes in epidermal morphology and corresponding protein level changes, we manually curated transcriptomics data for genes encoding proteins involved in epidermal differentiation and proliferation, including the epidermal differentiation complex, keratins, protease inhibitors, proteases, calcium binding proteins/AMP (antimicrobial peptides), proliferation, and late cornified envelope proteins (Figure 2A).[6,7] Statistical analysis of changes across the decades between 20's and 70's showed a pattern of elevated expression with age of differentiation associated genes in the photoexposed dorsal arm and face sites in most of these groups (Figure 2A, pink coloration). In contrast, genes associated with proliferation showed a decline in expression with age decades across all three body sites (Figure 2A, blue coloration). Trace profiles of representative probe sets from face of filaggrin (FLG), involucrin (IVL), arachidonate 12-lipoxygenase,12R (ALOX12B), loricrin (LOR), keratin 2 (KRT2), keratin 14 (KRT14), calmodulin-like protein 3 (CALML3), serine protease inhibitor Kazai-type 5 (SPINK5), cystatin B (CSTB), Krüppel-like factor 9 (KLF9), insulin like growth factor 1 receptor (IGF1R), and late cornified envelope 2C (LCE2C) show the relative expression changes across the decades (Figure 2B). Interestingly, the late cornified envelope proteins did not show as significant of a pattern when comparing across 20's and 70's but exhibits a significant increase up to the 50's and the reversal from 50's to 70's. To further visualize the gene expression profiles, we immunostained for several of these proteins in representative samples from young and old face and arm sites. Immunostaining for filaggrin showed heightened levels in the

upper granular/stratum corneum layers in a representative older age face site (Figure 2C) and to a lesser extent for involucrin and loricrin (Figure 2D and 2E). The basal keratin 14 marker showed a higher overall level of detection in a representative older age arm site (Figure 2F) and a modestly higher level of detection of the suprabasal marker keratin 10 (Figure 2G).

3.4 The IL-1RA/IL-1α ratio and IL-8 remain elevated across the decades in photoexposed facial skin, the *cis/trans* urocanic acid and 53BP1 DNA damage foci are detected in photoexposed sites, and epigenetic age is higher with age in photoexposed arm sites.

In addition to proteomics analysis on LCM-derived epidermal sections, we tested for the presence of the senescence-associated secretory phenotype (SASP) inflammatory biomarkers IL-8 and the IL-1RA/IL-1α ratio on the surface of skin.[8] Analysis of tape strip extractions showed the levels of both biomarkers were elevated in photoexposed face compared to dorsal arm and buttock sites (Figure 3A and 3B). Interestingly, the levels on face remained elevated across the age groups. It was surprising that we did not detect elevated levels of these cytokines in the photoexposed dorsal arm sites. To better understand this difference between the two sites, we analysed for the UV-sensitive metabolite ratio of *cis/trans*-urocanic acid. We showed a significant elevation in both face and arm compared to buttock consistent across the decades (Figure 3C). We also stained arm and buttock sites from both young and old for 53BP1, an indicator of DNA damage response induced by UV-irradiation.[9,10] Quantification showed

significantly more foci in the basal layer of aged arm compared to young, while very few foci were detected in buttock (Figure 3D-F). The buttock sites in either young or old did not show any significant increase in DNA damage. Additionally, we quantitated epigenetic age levels, which is based on DNA methylation levels from thousands of aging related locis.[11] We showed that both body sites showed elevated epigenetic age levels in the 60's when compared with the 30's, and significantly accelerated aging in arm sites compared to buttock sites (Figure 3G). The elevated levels of these photosensitive markers with age in arm and face sites support that both sites undergo a certain degree of photodamage. The muted levels of IL-8 and the IL-1RA/IL-1α ratio may be due to unknown physiological differences that merit further investigation.

3.5 Senescence and inflammation are elevated with age in photoexposed epidermis

The detection from facial skin surface of elevated levels of IL-8 which remains consistently high (Figure 3B) suggests that this site may present a higher senescence/inflammation rate than arm. As shown previously, we report that the senescence associated gene CDKN2A is elevated with age across all three body sites.[2] To better understand the correlation there may be between senescence, the heightened presence of the SASP-associated inflammatory biomarkers, and the epidermal morphological changes, we manually curated transcriptomics data for a subset of genes encoding for senescence and inflammatory associated proteins. We found an overall pattern of increased expression across the decades between 20's and 70's in both the

photoexposed arm and face sites, with more genes being upregulated in face (Figure 4A). In agreement, cyclin dependent kinase inhibitor 2A (CDKN2A), alpha-crystallin B chain (CRYAB), cytokine receptor type 2/IL8RB (CXCR2) were upregulated upon aging (Figure 4B). Similarly, several genes that have been reported to be reduced upon senescence (RBL2, SIRT, LMNB1) showed a general pattern of lowered expression (Figure 4A).[12-14] CDKN2A is known to encode several proteins involved in senescence and linkages to cancer, and aging, including $p16^{INK4A}$.[15-17] To further visualize the expression patterns, we immunostained biopsy sections from young and old face sites for $p16^{INK4a}$ and observed higher number of p16-positive cells in aged photoexposed facial skin throughout the basal and suprabasal layers (Figure 4C and 4D, yellow arrows).

3.6 An oxygen sensing/hypoxic fingerprint and metabolic reprograming increases with age in epidermis

The proteomics-based detection of elevated levels of several glycolytic enzymes in 60's aged epidermal arm LCM samples suggests the epidermis was undergoing a metabolic shift. A shift to glycolysis is a hallmark process of cells when exposed to hypoxic conditions. The morphological changes with age of increased stratum corneum thickness, decrease in rete ridge path length ratio, and less vasculature detection could impact oxygen bioavailability in the epidermis. Finally, the increased expression and protein detection of hemoglobin-α further suggests an oxygen sensing response by the epidermis. Thus, we manually curated from transcriptomics data a subset of genes

encoding proteins sensitive to oxygen tension or associated with cellular responses to hypoxia. These genes showed an increased expression pattern across the decades between 20's and 70's in arm, buttock, and face sites (Figure 5A, pink coloration). Consistent with this, genes encoding proteins known to negatively respond to hypoxia showed decreased expression across the decades, primarily in the photoexposed forearm and face sites (Figure 5A, blue coloration). Genes encoding glycolytic enzymes were also analysed and several genes were found to have elevated expression patterns across the decades between 20's and 70's in arm and face sites (Figure 5A, red coloration). To further illustrate the statistical findings, representative expression traces are shown for hypoxia inducible factor 1, subunit alpha (HIF1A, a master regulator of cellular response to hypoxic conditions), hemoglobin-β (HBB), heme oxygenase 1 (HMOX1), cystine/glutamate antiporter (SLC7A11), aldolase A (ALDOA), lysine demethylase 3A (KDM3A), lysine demethylase 5A (KDM5A), Sprouty homolog 2 (SPRY2), lactate dehydrogenase A (LDHA), and phosphoglucomutase 1 (PGM1) (Figure 5B). To further understand HIF1A and hemoglobin gene expression, we immunostained for HIF-1α and hemoglobin-α. A representative image shows staining of HIF-1α in nuclei of young face sites but higher expression was detected in older aged face sites (Figure 5C and 5D, red arrows). Representative images of hemoglobin-α staining in both arm and face sites highlight an elevated staining intensity throughout the upper granular/stratum corneum layers in arm (Figure 5E) and face (Figure 5F) from older individuals as compared to younger. Interestingly, there was no observable staining increase in the basal layer and through the dermis, further supporting that the presence of hemoglobin-α was epidermally derived and not erythroid.

4 DISCUSSION

The skin is the first line of defense protecting the body from environmental stressors such as solar radiation and pollution. Daily exposure to sunlight is one of the more significant environmental insults that induces DNA damage, oxidative stress, and inflammation in skin. Human skin must maintain robust repair capabilities to prevent cumulative damage triggered by these stressors. However, with age this ability is diminished, and the onset of senescence further hinders the skin's capacity to mitigate stress-induced inflammation and can lead to the presence of chronic low-level inflammation.[18] This phenotype is a key feature of inflammaging. The evidence for the presence of inflammaging in skin has been previously reviewed and it was highlighted that while there are clear signs of an inflammaging microenvironment in skin, further work is needed to better understand it's role on skin aging.[19]

To better understand the role of inflammaging on skin aging, we utilized a systems-biology based approach to investigate biological samples collected from photoprotected and exposed female body sites spanning 6 decades of age. A previous report found that patterns of gene expression accelerated with aging in Caucasian females and differed in a subgroup that appeared exceptionally youthful based on image analysis of facial appearance.[2] The current study focused on the epidermal skin compartment and employed a systems biology-based approach to increase our understanding and identify potential intervention strategies to mitigate premature aging. Our findings provide a body of evidence that photoexposed facial skin appears to be in an inflammaging microenvironment due to the presence of elevated chronic

inflammation which, in turn, could be a factor in part that leads to an imbalance in epidermal homeostasis starting in the 30's as measured via histology, transcriptomics, and proteomics (Figure 6). This suggests that targeting inflammation in younger aged skin may be a promising intervention approach to mitigate the molecular and morphological changes that lead to a photoaged appearance of skin and impact on underlying skin health.

The histomorphologic analysis in this study found that the epidermis undergoes significant changes with age, including stratum corneum thickening, implying that there may be a stronger barrier in older aged skin. While counter-intuitive, several reported studies have shown that trans-epidermal water loss values decrease in older aged subjects, suggesting that the barrier integrity improves with age.[20] However, the underlying health of the skin plays a role to ensure optimal repair response kinetics to damaging agents. Older aged skin has been shown to have a slower and weaker response profile to damage such as wounding and tape strip removal.[21, 22] We also show that with age the epidermis becomes thinner, the rete ridge path length flattens, and these changes correlate with changes in gene expression and protein levels associated with differentiation and proliferation, similar to *in vitro* data previously published.[23] Expression changes occur in a large proportion of genes encoding proteins associated with the epidermal complex, keratins, proteases, protease inhibitors, calcium bindings proteins/AMP, and late cornified envelope proteins. Additionally, these changes are more apparent in the photoexposed arm and face sites than the buttock site, confirming previous *in vitro* data where UVB irradiation led to increased levels of late differentiation markers.[24] This imbalance in differentiation and

proliferation processes appears to shift in the 30's and could be a factor in the observed morphological changes detected starting in the 40's. For example, the representative expression traces for FLG, LOR, ALOX12B, KRT2, CALML3, SPINK5, and CSTB all show a similar pattern of increased expression beginning in the 20's to 30's and continuing to increase across the decades. It is worth noting that some of these markers show alterations of this trend in the 50's, presumably due in part to hormonal changes as recorded in the previous study.[2] This is particularly highlighted in the respective traces presented as well as the overall expression patterns for the late cornified envelope proteins which showed significant changes in expression between the 20's and 50's but lost significance when comparing between the 20's and 70's. Several of the proteins expressed by these genes were also detected via proteomics profiling between the photoexposed arm of young and old subjects. A similar proteomics profiling has been reported in which the authors used tape strip collection to quantitate the levels of surface proteins associated with differentation.[25] Their findings are similar to the ones presented here with the exception that several proteins showed contrasting reduced levels in photoexposed skin compared to the elevated levels of those same proteins in our study. It should be pointed out that the age comparison between the 20's and 60's in this work was selected due to reversal of expression levels in the older 70's cohort. Future work will include additional analyses across all the age groups. Overall, there is an apparent correlation between the differentiation associated gene expression changes that begins in the 20's and correlates with the morphological changes that become significantly measurable starting in the 40's. This suggests an

imbalance in epidermal homeostasis which could impact its response profile to environmental insults and maintenance of normal cellular function.

To better understand the inflammatory and photoexposure status of the subjects in this study, we evaluated for the presence of inflammatory and photosensitive biomarkers isolated from the skin's surface. Detection of elevated levels of IL-8 has been shown to be elevated in eczema, atopic dermatitis, and psoriasis skin and in 3D skin models after UVB exposure. [26-28] We found elevated levels of IL-8 on photoexposed facial skin surface sites that remain elevated across age groups. The ratio of IL-1RA/IL-1α present on the skin's surface is known to be an indicator of underlying inflammation associated with skin dermatitis conditions and UV exposure.[29-31] Relative to impact of age and photoexposure on this inflammatory biomarker, it was reported that the IL-1RA/IL-1α ratio was elevated in photoexposed face compared to non-exposed upper inner arm and remained constant across age groups.[29] Relatedly, we show similar patterns when comparing between photoexposed face where the IL-RA/IL-lα ratio was consistently high and consistently low in photoprotected buttock sites across the decades. Surprisingly, we did not see an increase in these cytokines in photoexposed dorsal arm samples since we had previously reported there are significant histological indications of photoaging.[2] We show that several biomarkers associated with photoexposure are increased in arm sites, including the *cis/trans*-urocanic acid ratio, foci of the DNA damage response marker 53BP1 that is sensitive to UV exposure, and epigenetic age derived from methylation levels of DNA, an indicator of epigenetic aging.[11,32-34] These methylation patterns are similar to what has been previously reported where the biopsies were enzymatically separated into epidermis

and dermis fractions in contrast to LCM in our study.[35] Overall, this supports that the photoexposed arms undergo photodamage. We do not believe the lower levels of IL-8 or the IL-1RA/IL-1α ratio on photoexposed arm or buttock sites are an artefact since we performed the analysis in two independent experiments from duplicate tapes. The difference could reflect a dose response or a level of chronic exposure or, alternatively, facial skin is among the thinnest in the body and may be more susceptible to injury. While overall our results support the hypothesis that photoexposed skin is in a heightened state of inflammation, and that inflammation is present early in the 20's and remains persistent across the decades, future work is needed to understand the physiological relevance in photodamaged arms. Overall, the implications of this constant inflammatory pressure could be an indicator of skin inflammaging that leads to the changes in gene expression patterns and correlating protein levels in photoexposed skin.

We previously reported CDKN2A, a gene that encodes for proteins associated with senescence induction, to be elevated with age.[2] CDKN2A is known to encode for $p14^{ARF}$, $p15^{INK4B}$, and $p16^{INK4A}$, all of which are involved in senescence and play significant roles in cancer and aging, including in skin.[15-17] In the current study we wished to better understand this correlation beyond CDKN2A and performed a focused transcriptomics profiling of select genes encoding for proteins associated with regulation or induction of senescence in skin.[36] It has been established that photoexposure can cause keratinocytes to prematurely enter senescence and these cells can be characterized by secretion of an altered secretome called the senescence-associated

secretory phenotype (SASP), enriched with pro-inflammatory cytokines such as IL-6, IL-8, and IL-1β.[8]

The elevated skin surface levels of IL-8 early in the 20's age cohort on photoexposed face sites supports there may be an early onset of a SASP-associated phenotype in photodamaged facial skin. We see significant elevated levels of expression of genes encoding proteins associated with senescence in the photoexposed sites. For example, GLB1 encodes SA-β-gal (beta-galactosidase), a well-known biomarker of senescence in numerous tissues, including skin.[36] Several chemokine receptors were observed to increase in expression levels with age in the photoexposed arm and face sites. CXCR1 and CXCR2 encode receptor proteins that bind with IL-8 and showed elevated expression in both arm and face.[37] Interestingly this provides a potential correlation of inflammatory response with the elevated levels of IL-8 present on the skin's surface. A survey of candidate SASP components from a comparison between *in vitro* senescence models and *in vivo* tissue and fluid samples showed the elevated presence of CCL22, IL15, and MMP9 under senescent-impacted conditions.[38] The mammalian target of rapamycin (mTOR) is suggested to be a master regulator of metabolite sensing that impacts senescence induction and overall cellular aging.[39, 40] We show in both photoexposed epidermal sites an increase in mTOR expression levels with age (Figure 4A) that becomes significant in the 50's compared to the 20's for face (Figure 4B). CREG (cellular repressor of E1A-stimulated genes 1) co-expression with $p16^{INK4a}$ can further enhance senescence than either expressed alone.[41] Recently, CRYAB and HMOX1 have been proposed to be senolytic targets in humans cell models.[42] Interestingly, it was also demonstrated that HMOX1 expression

levels were increased during differentiation, which supports a similar correlation as measured in our study.[43] As reported here, we observe a significant increase in the expression patterns of these genes starting in the 30's and continuing into the 70's in photoexposed facial epidermis sites. In addition, we evaluated genes that encode proteins that mitigate senescence, including RBL2, SIRT1, SIRT3, SIR4, and TP53.[12,44-46] These show varying patterns of decreased expression in the epidermis of photoexposed sites with significance starting in the 50's and 60's. Finally, we immunostained for $p16^{INK4A}$ and detected nuclear localized puncti in both basal and spinous layers. Interestingly, it has been reported that $p16^{INK4a}$ is primarily detected in epidermal melanocytes by immunohistochemistry methods.[47] However, this may not be an exclusive scenario since it has also been reported that $p16^{INK4a}$ can be detected in keratinocytes in both basal and suprabasal layers, findings that are similar to ours.[48] These findings suggest that future work is needed to better define the role of this important senescence marker in the skin individual cell types.

In total, the data presented here supports that photoexposed skin is undergoing an accumulation of senescent cells with age. The chronic presence of the SASP factor IL-8 could be a causative indicator of senescence but further work is needed to establish cause and effect linked to the imbalance in differentiation-/proliferation and morphological changes.[49] The implications of skin undergoing these changes in inflammation and senescence due to photoexposure also has potential implications on overall body health. A recent review suggests there is a correlation between the accumulation of senescent cells in the skin and a negative impact on overall systemic health and longevity that occurs via the hypothalamic-pituitary-adrenal axis.[50] Future

work is planned to further correlate the gene expression and protein detection across individuals and body sites in this data set and from a recent clinical study.

Oxygenation of the epidermis occurs via passive diffusion from direct contact with atmospheric oxygen and from microcapillary beds intertwined underneath the basement membrane.[51] This may explain why the epidermis is considered to have a relatively low oxygen tension estimated to range between 0.3-8%, and why the epidermis could be considered hypoxic in contrast to the highly vascularized dermis where oxygen levels are estimated to be >7%.[51,52] The morphological changes measured in the epidermis with age suggested to us a further limitation of oxygen supply due to the longer diffusion path length through the thickened stratum corneum, as well as the reduced surface area interface with microcapillary beds from reduction of rete ridge undulation pattern. It has been previously reported that aging can lead to a measured increase in hypoxic-related response profiles.[53] That work utilized suction fluid blisters from young and older aged upper arms for transcriptomics profiling. In our study, we utilized the sensitivity of LCM dissection to localize the epidermis in both photoprotected and photoexposed skin sites for further investigation and an overall systems-biology body of evidence. The impact of a lowered oxygen tension in the epidermis is controlled in large part by hypoxia-inducible factor-1α (HIF-1α), a transcription factor and master regulator of cellular response to oxygen tension condition.[54] In addition to HIF-1α, an expanded transcriptomics profiling of select genes encoding proteins associated with regulation or responsiveness to oxygen tension changes or hypoxia supports our hypothesis that photoaged skin is transitioning into a more hypoxic microenvironment. For example, hypoxic conditions have been shown to

induce HMOX1 gene expression at 1% O_2 *in vitro* and 7% O_2 *in vivo* and this was mediated by HIF-1α activity.[55] Gene expression of the CXCL16-CXCR6 axis, CXCR4, and CXCL12 have been reported to be elevated under chronic hypoxic conditions.[56] PDSS1 encodes for decaprenyl diphosphate synthase subunit 1 and was recently identified as a member of a hypoxia signature in hepatocellular carcinoma cells.[57] We identified several genes whose expression patterns are negatively regulated under hypoxic conditions. Lysine demethylase 3A (KDM3A) has been reported to regulate PGC1α (PPARGC1A) and is inhibited under hypoxic conditions.[58] Silencing of SPRY2 gene expression was shown to correlate with elevated levels of HIF-1α.[59] Prolonged exposure to hypoxic conditions is known to shift cellular metabolism to a greater reliance on glycolysis due to the more anaerobic conditions.[60] We observed a similar shift based on elevated expression of genes encoding enzymes involved in glycolysis such as ALDOA, ENO1, LDHA, PGM1, and PKM. This was further supported by the detection of higher protein levels for ADLOA and PKM in older aged arm samples compared to younger aged samples. Expression for the glucose transporters SLC2A1, SLC2A3, and SLC7A11 were also elevated with age, which have been reported to be stimulated in response to hypoxia.[56,61] Interestingly, we detected elevated expression of hemoglobin-α and -β (HBA and HBB) and a numerically greater level of hemoglobin-α protein in older aged photoexposed arms. Of note, we did not see any significant staining for hemoglobin-α through the dermis and neither did we identify hemoglobin differences from proteomics of dermal sections (data not shown). While hemoglobin is well known for its role in O_2 and CO_2 gas exchange in red blood cells, an increasing number of non-erythroid tissues have been reported to endogenously express

hemoglobin.[62] The exact function of hemoglobin in non-erythroid tissue is not clear but it has been speculated it could include regulation of heme, iron and oxygen levels.[63] It has also been proposed that hemoglobin plays a role in response to oxidative stress by helping protect against ROS damage.[64] Overall, the significant increase in expression of genes associated with hypoxia and glycolytic enzymes suggests a phenotype reflecting a hypoxic microenvironment in photoexposed skin and, to a weaker extent, in non-exposed skin. The reported range of O_2 tension in the epidermis has a broad range between 0.3-8%[51,52], and we would propose that in this study cohort the tension was significantly lower in the older age group compared with the younger group. Further work is needed to validate these findings with quantitation of differences in oxygen content in the epidermal compartment as a function of age and photoexposure.

Limitations exist in this study since it is not clear on the causal relationship between the molecular changes ascribed and the cascade across the decades to the morphological changes.

5 CONCLUSIONS

In summary, this systems biology-based approach to analyse inflammatory and photosensitive biomarkers, proteomics, transcriptomics, and immunostaining strongly suggests that photoexposed facial skin is undergoing inflammaging that begins as early as in the 20's and that multiple biologic pathways are affected in this process. We propose that the chronic presence of inflammation and SASP early in age may contribute to the molecular reprogramming, imbalance of epidermal homeostasis, and morphological changes. The presence of heightened senescence, oxygen

sensing/hypoxic response, epigenetic drift, and metabolic shift may also play roles leading to this imbalance. While this work provides further evidence on the role of senescence and inflammation in impacting aging in photoexposed skin, further evidence is still required.[65, 66] Finally, the detection of non-erythroid-derived hemoglobin in the epidermis is a novel finding that merits further evaluation on its function and role in skin biology and aging.

ACKNOWLEDGEMENTS

We acknowledge the assistance of John C. Bierman in facilitating tape strip analysis.

CONFLICT OF INTEREST

The authors state no conflict of interest. XY, CN, WG, and YCC are full-time employees of Zymo Research Corporation. BBJ, YMD, and JEO are full-time employees of The Procter & Gamble Company.

AUTHOR CONTRIBUTIONS

BBJ, CYRT, CYH, TTL, XY, LC, SP, SB, OD, and JEO conceived the experiments; BBJ, CYRT, CYH, ALS, TTL, XY, CN, WG, YCC, YMD, LC, and PSG performed experiments and analysed the data. JEO wrote the manuscript. All authors reviewed/edited the manuscript.

DATA AVAILABILITY STATEMENT

The data that support the findings of this study are available from the corresponding author upon reasonable request.

ORCID

John E. Oblong https://orcid.org/0000-0001-7628-6242

REFERENCES

1. Yaar M, Gilchrest BA. Photoaging: mechanism, prevention and therapy. *Br J Dermatol*. 2007; **157**:874-887.

2. Kimball AB, Alora-Palli MB, Tamura M, Mullins LA, Soh C, Binder RL, Houston NA, Conley ED, Tung JY, Annunziata NE, Bascom CC, Isfort RJ, Jarrold BB, Kainkaryam R, Rocchetta HL, Swift DD, Tiesman JP, Toyama K, Xu J, Yan X, Osborne R. Age-induced and photoinduced changes in gene expression profiles in facial skin of Caucasian females across 6 decades of age. *J Am Acad Dermatol.* 2018; **78**(1):29-39.

3. Holthöfer H, Virtanen I, Kariniemi AL, Hormia M, Linder E, Miettinen A. Ulex europaeus I lectin as a marker for vascular endothelium in human tissues. *Lab Invest.* 1982; **47**(1): 60-66.

4. Bennett MF, Robinson MK, Baron ED, Cooper KD. Skin immune systems and inflammation: protector of the skin or promoter of aging? *J Inv Derm Symp Proc.* 2008; **13:1**5-19.

5. Zhuang Y, Lyga J. Inflammaging in skin and other tissues – the roles of complement system and macrophage. *Inflamm Allergy Drug Targets.* 2014; **13**:153-161.

6. Kypriotou M, Huber M, Hohl D. The human epidermal differentiation complex: cornified envelope precursors, S100 proteins and the 'fused genes' family. Exp Dermatol. 2012 Sep;21(9):643-9. doi:

7. Rousselle P, Gentilhomme E, Neveux Y. (2017) Markers of Epidermal Proliferation and Differentiation. In: Humbert P, Fanian F, Maibach H, Agache P. (eds) Agache's Measuring the Skin. Springer, Cham. https://doi.org/10.1007/978-3-319-32383-1_37.

8. Fitsiou E, Pulido T, Campisi J, Alimirah F, Demaria M. Cellular senescence and the senescence-associated secretory phenotype as drivers of skin photoaging. *J Invest Dermatol.* 2021; **141**(4S):1119-1126.

9. Shibata A, Jeggo PA. Roles for 53BP1 in the repair of radiation-induced DNA double strand breaks. *DNA Repair (Amst).* 2020; **93**:102915.

10. Lee, J. W., Ratnakumar, K., Hung, K. F., Rokunohe, D., & Kawasumi, M. (2020). Deciphering UV-induced DNA Damage Responses to Prevent and Treat Skin Cancer. *Photochemistry and photobiology*, *96*(3), 478–499.

11. Horvath S. DNA methylation age of human tissues and cell types. *Genome Biol.* 2013; **14**(10):R115.

12. Xu C, Wang L, Fozouni P. *et al.* SIRT1 is downregulated by autophagy in senescence and ageing. *Nat Cell Biol.* 2020; **22**: 1170–1179.

13. Freund A, Laberge RM, Demaria M, Campisi J. Lamin B1 loss is a senescence-associated biomarker. *Mol Biol Cell*. 2012; **23**(11):2066-2075.

14. Dreesen O, Chojnowski A, Ong PF, Zhao TY, Common JE, Lunny D, Lane EB, Lee SJ, Vardy LA, Stewart CL, Colman A. Lamin B1 fluctuations have differential effects on cellular proliferation and senescence. *J Cell Biol.* 2013; **200**(5):605-617.

15. Ressler S, Bartkova J, Niederegger H, Bartek J, Scharffetter-Kochanek K, Jansen-Dürr P, Wlaschek M. $p16^{INK4A}$ is a robust in vivo biomarker of cellular aging in human skin. *Aging Cell.* 2006; **5**(5):379-389.

16. Waaijer ME, Parish WE, Strongitharm BH, van Heemst D, Slagboom PE, de Craen AJ, Sedivy JM, Westendorp RG, Gunn DA, Maier AB. The number of $p16^{INK4a}$ positive cells in human skin reflects biological age. *Aging Cell.* 2012;**11**(4):722-725.

17. LaPak KM, Burd CE. The Molecular Balancing Act of $p16^{INK4a}$ in Cancer and Aging *Mol Cancer Res* 2014; **12**(2):167-183.

18. Ho CY, Dreesen O. Faces of cellular senescence in skin aging. *Mech Ageing Dev.* 2021; **198**:111525.

19. Pilkington SM, Bulfone-Paus S, Griffiths CEM, Watson REB. Inflammaging and the Skin. *J Invest Dermatol.* 2021; **141**(4S):1087-1095.

20. Wilhelm KP, Cua AB, Maibach HI. Skin aging. Effect on transepidermal water loss, stratum corneum hydration, skin surface pH, and casual sebum content. *Arch Dermatol.* 1991; **127**(12):1806-1809.

21. Ghadially R, Brown BE, Sequeira-Martin SM, Feingold KR, Elias PM. The aged epidermal permeability barrier. Structural, functional, and lipid biochemical abnormalities in humans and a senescent murine model. *J Clin Invest.* 1995; **95**(5):2281-2290.

22. Gosain A, DiPietro LA. Aging and wound healing. *World J Surg.* 2004; **28**(3):321-326.

23. Tan CL, Chin T, Tan CYR, Rovito HA, Quek LS, Oblong JE, Bellanger S. Nicotinamide Metabolism Modulates the Proliferation/Differentiation Balance and Senescence of Human Primary Keratinocytes. *J Invest Dermatol.* 2019; **139**(8):1638-1647.

24. Tan CYR, Tan CL, Chin T, Morenc M, Ho CY, Rovito HA, Quek LS, Soon AL, Lim JSY, Dreesen O, Oblong JE, Bellanger S. Nicotinamide Prevents UVB- and Oxidative Stress–Induced Photoaging in Human Primary Keratinocytes. *J Invest Dermatol*. 2022; **142**(6):1670-1681.

25. Voegeli R, Monneuse JM, Schoop R, Summers B, Rawlings AV. The effect of photodamage on the female Caucasian facial stratum corneum corneome using mass spectrometry-based proteomics. Int *J Cosmet Sci.* 2017; **39**(6):637-652.

26. Sticherling M, Bornscheuer E, Schröder J-M, Christophers E. Localization of NAP-1/IL-8 immunoreactivity in normal and psoriatic skin. *J Invest Dermatol* 1991; **96**: 26-30.

27. Sticherling M, Bornscheuer E, Schröder JM, Christophers E. Immunohistochemical studies on NAP-1/IL-8 in contact eczema and atopic dermatitis. *Arch Dermatol Res* 1992; **284**: 82-85.

28. Amarbayasgalan T, Takahashi H, Dekio I, Morita E. Interleukin-8 content in the stratum corneum as an indicator of the severity of inflammation in the lesions of atopic dermatitis. *Int Arch Allergy Immunol.* 2013; **160**(1):63-74.

29. Hirao T, Aoki H, Yoshida T, Sato Y, Kamoda H. Elevation of interleukin 1 receptor antagonist in the stratum corneum of sun-exposed and ultraviolet B-irradiated human skin. *J Invest Dermatol.* 1996;**106**(5):1102-1107.

30. Terui T, Hirao T, Sato Y, Uesugi T, Honda M, Iguchi M, Matsumura N, Kudoh K, Aiba S, Tagami H. An increased ratio of interleukin-1 receptor antagonist to interleukin-1alpha in inflammatory skin diseases. *Exp Dermatol.* 1998; **7**(6):327-334.

31. Perkins MA, Osterhues MA, Farage MA, Robinson MK. A non-invasive method to assess skin irritation and compromised skin conditions using simple tape adsorption of molecular markers of inflammation. *Skin Res Technol.* 2001; **7**(4):227-237.

32. de Fine Olivarius F, Wulf HC, Therkildsen P, Poulsen T, Crosby J, Norval M. Urocanic acid isomers: relation to body site, pigmentation, stratum corneum thickness and photosensitivity. *Arch Dermatol Res.* 1997; **289**(9):501-505.

33. Uehara F, Miwa S, Tome Y, Hiroshima Y, Yano S, Yamamoto M, Efimova E, Matsumoto Y, Maehara H, Bouvet M, Kanaya F, Hoffman RM. Comparison of UVB and UVC effects on the DNA damage-response protein 53BP1 in human pancreatic cancer. *J Cell Biochem.* 2014; **115**(10):1724-1728.

34. Bártová E, Legartová S, Dundr M, Suchánková J. A role of the 53BP1 protein in genome protection: structural and functional characteristics of 53BP1-dependent DNA repair. *Aging (Albany NY)*. 2019; **11**(8):2488-2511.

35. Grönniger E, Weber B, Heil O, Peters N, Stäb F, Wenck H, Korn B, Winnefeld M, Lyko F. Aging and chronic sun exposure cause distinct epigenetic changes in human skin. *PLoS Genet.* 2010; **6**(5):e1000971.

36. Wang AS, Dreesen O. Biomarkers of Cellular Senescence and Skin Aging. *Front Genet.* 2018; **9**:247.

37. Varney ML, Johansson SL, Singh RK. Distinct expression of CXCL8 and its receptors CXCR1 and CXCR2 and their association with vessel density and aggressiveness in malignant melanoma. *Am J Clin Pathol*. 2006; **125**(2):209-216.

38. Schafer MJ, Zhang X, Kumar A, Atkinson EJ, Zhu Y, Jachim S, Mazula DL, Brown AK, Berning M, Aversa Z, Kotajarvi B, Bruce CJ, Greason KL, Suri RM, Tracy RP, Cummings SR, White TA, LeBrasseur NK. The senescence-associated secretome as an indicator of age and medical risk. *JCI Insight*. 2020; **5**(12):e133668.

39. Xu S, Cai Y, Wei Y. mTOR Signaling from Cellular Senescence to Organismal Aging. *Aging Dis.* 2013; **5**(4):263-273.

40. Huang K, Fingar DC. Growing knowledge of the mTOR signaling network. *Semin Cell Dev Biol.* 2014; **36**:79-90.

41. Moolmuang B, Tainsky MA. CREG1 enhances $p16^{INK4a}$-induced cellular senescence. *Cell Cycle*. 2011; **10**(3):518-530.

42. Limbad C, Doi R, McGirr J, Ciotlos S, Perez K, Clayton ZS, Daya R, Seals DR, Campisi J, Melov S. Senolysis induced by 25-hydroxycholesterol targets CRYAB in multiple cell types. *iScience*. 2022; **25**(2):103848.

43. Numata I, Okuyama R, Memezawa A, Ito Y, Takeda K, Furuyama K, Shibahara S, Aiba S. Functional expression of heme oxygenase-1 in human differentiated epidermis and its regulation by cytokines. *J Invest Dermatol.* 2009; **129**(11):2594-2603.

44. Alessio N, Bohn W, Rauchberger V, Rizzolio F, Cipollaro M, Rosemann M, Irmler M, Beckers J, Giordano A, Galderisi U. Silencing of RB1 but not of RB2/P130 induces cellular senescence and impairs the differentiation potential of human mesenchymal stem cells. Cell Mol Life Sci. 2013 May;70(9):1637-51.

45. Kida Y, Goligorsky MS. Sirtuins, Cell Senescence, and Vascular Aging. *Can J Cardiol.* 2016; **32**(5):634-641.

46. Kim RH, Kang MK, Kim T, Yang P, Bae S, Williams DW, Phung S, Shin KH, Hong C, Park NH. Regulation of p53 during senescence in normal human keratinocytes. *Aging Cell*. 2015; **14**(5):838-846.

47. Victorelli S, Lagnado A, Halim J, Moore W, Talbot D, Barrett K, Chapman J, Birch J, Ogrodnik M, Meves A, Pawlikowski JS, Jurk D, Adams PD, van Heemst D, Beekman M, Slagboom PE, Gunn DA, Passos JF. Senescent human melanocytes drive skin ageing via paracrine telomere dysfunction. *EMBO J.* 2019; **38**(23):e101982.

48. Pavey S, Conroy S, Russell T, Gabrielli B. Ultraviolet radiation induces p16CDKN2A expression in human skin. Cancer Res. 1999 Sep 1;59(17):4185-9

49. Demaria M, Desprez PY, Campisi J, Velarde MC. Cell autonomous and non-autonomous effects of senescent cells in the skin. *J Invest Dermatol.* 2015; **135**(7):1722-1726.

50. Franco AC, Aveleira C, Cavadas C. Skin senescence: mechanisms and impact on whole-body aging. *Trends Mol Med.* 2022; **28**(2):97-109.

51. Stücker M, Struk A, Altmeyer P, Herde M, Baumgärtl H, Lübbers DW. The cutaneous uptake of atmospheric oxygen contributes significantly to the oxygen supply of human dermis and epidermis. *J Physiol.* 2002; **538**:985-994.

52. Evans SM, Schrlau AE, Chalian AA, Zhang P, Koch CJ. Oxygen levels in normal and previously irradiated human skin as assessed by EF5 binding. *J Invest Dermatol.* 2006; **126**(12):2596

53. Prahl S, Kueper T, Biernoth T, Wöhrmann Y, Münster A, Fürstenau M, Schmidt M, Schulze C, Wittern KP, Wenck H, Muhr GM, Blatt T. Aging skin is functionally anaerobic: importance of coenzyme Q10 for anti aging skin care. *Biofactors.* 2008; **32**(1-4):245-255.

54. Rezvani HR, Ali N, Nissen LJ, Harfouche G, de Verneuil H, Taïeb A, Mazurier F. HIF-1α in epidermis: oxygen sensing, cutaneous angiogenesis, cancer, and non-cancer disorders. *J Invest Dermatol.* 2011; **131**(9):1793-1805.

55. Lee PJ, Jiang BH, Chin BY, Iyer NV, Alam J, Semenza GL, Choi AM. Hypoxia-inducible factor-1 mediates transcriptional activation of the heme oxygenase-1 gene in response to hypoxia. *J Biol Chem.* 1997; **272**(9):5375-5381.

56. Korbecki J, Kojder K, Kapczuk P, Kupnicka P, Gawrońska-Szklarz B, Gutowska I, Chlubek D, Baranowska-Bosiacka I. The Effect of Hypoxia on the Expression of CXC Chemokines and CXC Chemokine Receptors-A Review of Literature. *Int J Mol Sci.* 2021; **22**(2):843.

57. Zhang B, Tang B, Gao J, Li J, Kong L, Qin L. A hypoxia-related signature for clinically predicting diagnosis, prognosis and immune microenvironment of hepatocellular carcinoma patients. *J Transl Med*. 2020; **18**(1):342.

58. Qian X, Li X, Shi Z, Bai X, Xia Y, Zheng Y, Xu D, Chen F, You Y, Fang J, Hu Z, Zhou Q, Lu Z. KDM3A Senses Oxygen Availability to Regulate PGC-1α-Mediated Mitochondrial Biogenesis. *Mol Cell.* 2019; **76**(6):885-895.

59. Hicks KC, Patel TB. Sprouty2 Protein Regulates Hypoxia-inducible Factor-α (HIFα) Protein Levels and Transcription of HIFα-responsive Genes. *J Biol Chem*. 2016; **291**(32):16787-16801.

60. Czyzyk-Krzeska MF. Molecular aspects of oxygen sensing in physiological adaptation to hypoxia. *Respir Physiol*. 1997; **110**(2-3):99-111.

61. Airley RE, Mobasheri A. Hypoxic regulation of glucose transport, anaerobic metabolism and angiogenesis in cancer: novel pathways and targets for anticancer therapeutics. *Chemotherapy*. 2007; **53**(4):233-256.

62. Saha D, Patgaonkar M, Shroff A, Ayyar K, Bashir T, Reddy KV. Hemoglobin expression in nonerythroid cells: novel or ubiquitous? *Int J Inflam.* 2014; 803237.

63. H. Dassen R, Kamps C, Punyadeera F, Dijcks A, de Goeij A, Ederveen G, Dunselman P, Groothuis. Haemoglobin expression in human endometrium, *Human Reproduction*, 2008; **23**(3): 635–641.

64. Saha D, Koli S, Reddy KVR. Transcriptional regulation of Hb-α and Hb-β through nuclear factor E2-related factor-2 (Nrf2) activation in human vaginal cells: A novel mechanism of cellular adaptability to oxidative stress. *Am J Reprod Immunol.* 2017; **77**(6).

65. Low E, Alimohammadiha G, Smith LA, Costello LF, Przyborski SA, von Zglinicki T, Miwa S. How good is the evidence that cellular senescence causes skin ageing? *Ageing Res Rev*. 2021; **71**:101456.

66. Lee YI, Choi S, Roh WS, Lee JH, Kim TG. Cellular Senescence and Inflammaging in the Skin Microenvironment. *Int J Mol Sci*. 2021; **22**(8):3849.

Early onset of senescence and imbalanced epidermal homeostasis across the decades in photoexposed human skin: fingerprints of inflammaging.

~~Inflammaging in human photoexposed skin: Early onset of senescence and imbalanced epidermal homeostasis across the decades.~~

Bradley B. Jarrold[1], Christina Yan Ru Tan[2], Chin Yee Ho[2], Ai Ling Soon[2], TuKiet T. Lam[3], Xiaojing -Yang[4], Calvin Nguyen[4], Wei Guo[4], Yap Ching Chew[4], Yvonne M. DeAngelis[1], Lydia Costello[5], Paola De Los Santos Gomez[5], Stefan Przyborski[5], Sophie Bellanger[2], Oliver Dreesen[2], Alexa B. Kimball[6], and John E. Oblong[1]

[1]The Procter & Gamble Company, Cincinnati, OH, USA; [2]A*STAR Skin Research Labs, Singapore, Singapore; [3]Keck MS & Proteomics Resource, Yale School of Medicine, New Haven, CT, USA; [4]Zymo Research Corporation, Irvine, CA, USA; [5]Durham University, Durham, UK; [6]Beth Israel Deaconess Medical Center and Harvard Medical School, Boston, MA, USA

Correspondence: John E. Oblong, The Procter & Gamble Company, Cincinnati, OH, 45040, USA. E-mail: oblong.je@pg.com

Short title: Chronic inflammation remains elevated across decades in a 20's to 70's year old cohort.

Keywords: Epidermis, photoexposed, inflammation, inflammaging, epidermal morphology, senescence, differentiation, glycolysis, hypoxia, and epigenetics

Abbreviation list

LCM: laser capture microdissection

SASP: senescence-associated secretory phenotype

DEJ: dermal epidermal junction

UEA-1: *Ulex Europaeus*-I Lectin

53BP1: p53-binding protein 1

IL-8: interleukin-8

IL-1α: interleukin-1α

IL-1RA: interleukin-1 receptor antagonist

FLG: filaggrin

INV: involucrin

ALOX12B: arachidonate 12-lipoxygenase,12R

LOR: loricrin

KRT2: keratin 2

KRT14: keratin 14

CALML3: calmodulin-like protein 3

SPINK5: serine protease inhibitor Kazai-type 5

CSTB: cystatin B

KLF9: Krüppel-like factor 9

IGF1R: insulin like growth factor 1 receptor

LCE2C: late cornified envelope 2C

CAPN1: calpain 1

CDKN2A: cyclin dependent kinase inhibitor 2A

CRYAB: alpha-crystallin B chain

CXCR2: cytokine receptor type 2/IL8RB

mTOR: mammalian target of rapamycin

RBL2: retinoblastoma-like protein 2

SIRT1: sirtuin 1

HIF1α: hypoxia inducible factor 1, subunit alpha

HBA: hemoglobin-α

HBB: hemoglobin-β

HMOX1: heme oxygenase 1

SLC7A11: cystine/glutamate antiporter

ALDOA: aldolase A

KDM3A: lysine demethylase 3A

KDM5A: lysine demethylase 5A

SPRY2: Sprouty homolog 2

LDHA: lactate dehydrogenase A

PGM1: phosphoglucomutase 1

ABSTRACT

Inflammaging is a theory of aging which purports that low-level chronic inflammation leads to cellular dysfunction and premature aging of surrounding tissue. Skin is susceptible to inflammaging because it is the first line of defense from the environment, particularly solar radiation. To better understand the impact of aging and photoexposure on epidermal biology, we performed a systems biology-based analysis of photoexposed face and arm, and photoprotected buttock sites, from women between the ages of 20's to 70's. Biopsies were analyzed by histology, transcriptomics, and proteomics and skin surface biomarkers collected from tape strips. We identified morphological changes with age of epidermal thinning, rete ridge pathlength loss, and stratum corneum thickening. The SASP biomarkers IL-8 and IL-1RA/IL1-α were consistently elevated in face across age and *cis/trans*-urocanic acid were elevated in arms and face with age. In older arms, the DNA damage response biomarker 53BP1 showed higher puncti numbers in basal layers and epigenetic aging was accelerated. Genes associated with differentiation and senescence showed increasing expression in the 30's whereas genes associated with hypoxia and glycolysis increased in the 50's. Proteomics comparing 60's vs 20's confirmed elevated levels of differentiation and glycolytic related proteins. Representative immunostaining for proteins of differentiation, senescence, and oxygen sensing/hypoxia ~~shows~~ showed similar relationships. This systems biology-based analysis provides a body of evidence that young photoexposed skin is undergoing inflammaging. We propose the presence of chronic inflammation in young skin contributes to an imbalance of epidermal homeostasis that leads to a prematurely aged appearance during later life.

1 INTRODUCTION

The skin is one of the largest organs of the human body, providing protection from external insults such as solar radiation, pollution, chemicals, and particulate matter. Like all organs of the body, the skin is susceptible to aging, resulting in structural and functional changes which may be accelerated further by environmental insults.[1] This premature aging of skin leads to cellular and morphological changes that accumulate over time and ultimately affect the skin's appearance, functionality, and homeostatic state. This homeostasis is dependent on an organized and timely renewal process, initiated by basal keratinocytes which proliferate and differentiate to ultimately transform into corneocytes that comprise the stratum corneum. An imbalance in this process has implications on skin's appearance, health, and response to stress. Thus, it is essential to understand these changes to identify mechanistic intervention targets that would prevent and repair premature aging and maintain skin health and appearance.

We previously reported findings from a large base study that evaluated biopsies collected from photoexposed face and dorsal forearms as well as photoprotected buttock sites of Caucasian females across age decades spanning 20's to the 70's, demonstrating that age impacts a wide range of molecular processes in skin.[2] Given that a low grade chronic inflammatory state is hypothesized to be a significant contributor to premature aging in the inflammaging theory, we asked whether this phenomenon could be observed in our previously reported skin biopsy study and investigated its potential impact on epidermal biology and homeostasis. A systems biology-based analysis of skin surface biomarkers, transcriptomics, proteomics, metabolomics, histology, and immunostaining confirmed that there is underlying chronic

inflammation in photoexposed face skin that remains elevated across the decades. Primarily in photoexposed skin, we found ~~there is~~ an imbalance in epidermal homeostasis beginning in the 20's to 30's and elevation of senescence~~-~~-related components in the 30's to 40's. A subsequent increase of oxygen sensing/hypoxia and metabolic shift towards glycolysis occurs in the 50's. Additionally, there is a higher epigenetic aging rate in 60's when comparing to the 30's and is further elevated by photoexposure. Based on these findings, we propose that photoexposed skin undergoes inflammaging which may play a role in the molecular and morphological changes that ultimately lead to a photoaged appearance and less healthy state of skin.

2 MATERIALS AND METHODS

The detailed protocols and statistical analysis are described in Supplemental Materials and Methods.

3 RESULTS

3.1 Age-associated changes in epidermal morphology

We first performed a histomorphometric analysis of the structural compartments of the epidermis from buttock, arm, and face sites across age groups. With age, the overall thickness of the stratum corneum ~~increased~~ increases (Figure 1A) whereas the epidermal layer becomes thinner (Figure 1B), and the rete ridge path length ratio decreases (Figure 1C). Comparison of the mean data between the 20's and each decade showed that these changes become statistically significant in the older age

groups (Supplemental Table 1). A representative histological stain from a 20's and a 60's year old face highlights these structural changes (Figure 1D). In an older age sample, we observed relatively lower detection of microcapillary structures using staining against UEA-1, a lectin that binds to endothelial related cells.[3] A representative image shows the differential staining pattern below the basement membrane (Figure 1E, white arrows) as well as staining in the stratum granulosum and corneum. This pattern is similar to what has been previously reported in skin.[3] The structural changes of thickening of the stratum corneum and the thinning of the epidermis suggest an imbalance between proliferation and differentiation that changes with age across all body sites.

3.2 Proteomics analysis shows elevated presence of proteins associated with differentiation and glycolysis in 60's aged dorsal forearm epidermis over 20's age group.

To better understand these measured changes in epidermal structure with age, LCM isolated epidermal sections from 20's and 60's dorsal arms were processed and analysed by label free quantitative mass spectrometry. Out of 367 proteins identified, 83 showed a significant difference (p<0.1) in levels when comparing between the two age groups (Supplemental Table 2). Of the 83 proteins, 24 proteins were associated with epidermal differentiation and metabolism/oxygen sensing (Table 1). 23 of these had a similar directional relationship with their representative gene expression pattern with age. The exception is calpain 1 (CAPN1) which showed no significant change in

expression levels across the decades (data not shown). Interestingly, we also detected a higher numerical level of hemoglobin-α (p=0.092) and hemoglobin-β (p=0.134, data not shown) present in the older group.

3.3 Imbalance in epidermal differentiation/proliferation increases with age in photoexposed epidermis.

To further understand the age-associated changes in epidermal morphology and corresponding protein level changes, we manually curated transcriptomics data for genes encoding ~~for~~ proteins involved in epidermal differentiation and proliferation, including the epidermal differentiation complex, keratins, protease inhibitors, proteases, calcium binding proteins/AMP (antimicrobial peptides), proliferation, and late cornified envelope proteins (Figure 2A).[6,7] Statistical analysis of changes across the decades between 20's and 70's showed a pattern of elevated expression with age of differentiation associated genes in the photoexposed dorsal arm and face sites in most of these groups (Figure 2A, pink coloration). In contrast, genes associated with proliferation showed a decline in expression with age decades across all three body sites (Figure 2A, blue coloration). Trace profiles of representative probe sets from face of filaggrin (FLG), involucrin (IVL), arachidonate 12-lipoxygenase,12R (ALOX12B), loricrin (LOR), keratin 2 (KRT2), keratin 14 (KRT14), calmodulin-like protein 3 (CALML3), serine protease inhibitor Kazai-type 5 (SPINK5), cystatin B (CSTB), Krüppel-like factor 9 (KLF9), insulin like growth factor 1 receptor (IGF1R), and late cornified envelope 2C (LCE2C) show the relative expression changes across the decades

(Figure 2B). Interestingly, the late cornified envelope proteins did not show as significant of a pattern when comparing across 20's and 70's but exhibits a significant increase up to the 50's and the reversal from 50's to 70's. To further visualize the gene expression profiles, we immunostained for several of these proteins in representative samples from young and old face and arm sites. Immunostaining for filaggrin showed heightened levels in the upper granular/stratum corneum layers in a representative older age face site (Figure 2C) and to a lesser extent for involucrin and loricrin (Figure 2D and 2E). The basal keratin 14 marker showed a higher overall level of detection in a representative older age arm site (Figure 2F) and a modestly higher level of detection of the suprabasal marker keratin 10 (Figure 2G).

3.4 The IL-1RA/IL-1α ratio and IL-8 remain elevated across the decades in photoexposed facial skin, the *cis/trans* urocanic acid and 53BP1 DNA damage foci are detected in photoexposed sites, and epigenetic age is higher with age in photoexposed arm sites.

In addition to proteomics analysis on LCM-derived epidermal sections, we tested for the presence of the senescence-associated secretory phenotype (SASP) inflammatory biomarkers IL-8 and the IL-1RA/IL-1α ratio on the surface of skin.[8] Analysis of tape strip extractions showed the levels of both biomarkers were elevated in photoexposed face compared to dorsal arm and buttock sites (Figure 3A and 3B). Interestingly, the levels on face remained elevated across the age groups. It was surprising that we did not detect elevated levels of these cytokines in the photoexposed dorsal arm sites. To

better understand this difference between the two sites, we analysed for the UV-sensitive metabolite ratio of *cis/trans*-urocanic acid. We showed a significant elevation in both face and arm compared to buttock ~~site and was~~ consistent across the decades (Figure 3C). We also stained arm and buttock sites from both young and old for 53BP1, an indicator of DNA damage response induced by UV-irradiation.[9,10] Quantification showed significantly more foci in the basal layer of aged arm compared to young, while very few foci were detected in buttock (Figure 3D-F). The buttock sites in either young or old did not show any significant increase in DNA damage. Additionally, we quantitated epigenetic age levels, which is based on DNA methylation levels from thousands of aging related locis.[11] We showed that both body sites showed elevated epigenetic age levels in the 60's when compared with the 30's, and significantly accelerated aging in arm sites compared to buttock sites (Figure 3G). The elevated levels of these photosensitive markers with age in arm and face sites support that both sites undergo a certain degree of photodamage. The muted levels of IL-8 and the IL-1RA/IL-1α ratio may be due to unknown physiological differences that merit further investigation.

3.5 Senescence and inflammation are elevated with age in photoexposed epidermis

The detection from facial skin surface of elevated levels of IL-8 which remains consistently high (Figure 3B) suggests that this site may present a higher senescence/inflammation rate than arm. As shown previously, we report that the

senescence associated gene CDKN2A ~~was~~ is elevated with age across all three body sites.[2] To better understand the correlation there may be between senescence, the heightened presence of the SASP-associated inflammatory biomarkers, and the epidermal morphological changes, we manually curated transcriptomics data for a subset of genes encoding for senescence and inflammatory associated proteins. We found an overall pattern of increased expression across the decades between 20's and 70's in both the photoexposed arm and face sites, with more genes being upregulated in face (Figure 4A). In agreement, cyclin dependent kinase inhibitor 2A (CDKN2A), alpha-crystallin B chain (CRYAB), cytokine receptor type 2/IL8RB (CXCR2) were upregulated upon aging (Figure 4B). Similarly, several genes that have been reported to be reduced upon senescence (RBL2, SIRT, LMNB1) showed a general pattern of lowered expression (Figure 4A).[12-14] CDKN2A is known to encode ~~for~~ several proteins involved in senescence and linkages to cancer, and aging, including $p16^{INK4A}$.[15-17] To further visualize the expression patterns, we immunostained biopsy sections from young and old face sites for $p16^{INK4a}$ and observed higher number of p16-positive cells in aged photoexposed facial skin throughout the basal and suprabasal layers (Figure 4C and 4D, yellow arrows).

3.6 An oxygen sensing/hypoxic fingerprint and metabolic reprograming increases with age in epidermis

The proteomics-based detection of elevated levels of several glycolytic enzymes in 60's aged epidermal arm LCM samples suggests the epidermis was undergoing a metabolic

shift. A shift to glycolysis is a hallmark process of cells when exposed to hypoxic conditions. The morphological changes with age of increased stratum corneum thickness, decrease in rete ridge path length ratio, and less vasculature detection could impact oxygen bioavailability in the epidermis. Finally, the increased expression and protein detection of hemoglobin-α further suggests an oxygen sensing response by the epidermis. Thus, we manually curated from transcriptomics data a subset of genes encoding ~~for~~ proteins sensitive to oxygen tension or associated with cellular responses to hypoxia. These genes showed an increased expression pattern across the decades between 20's and 70's in arm, buttock, and face sites (Figure 5A, pink coloration). Consistent with this, genes encoding ~~for~~ proteins known to negatively respond to hypoxia showed decreased expression across the decades, primarily in the photoexposed forearm and face sites (Figure 5A, blue coloration). Genes encoding ~~for~~ glycolytic enzymes were also analysed and several genes were found to have elevated expression patterns across the decades between 20's and 70's in arm and face sites (Figure 5A, red coloration). To further illustrate the statistical findings, representative expression traces are shown for hypoxia inducible factor 1, subunit alpha (HIF1A, a master regulator of cellular response to hypoxic conditions), hemoglobin-β (HBB), heme oxygenase 1 (HMOX1), cystine/glutamate antiporter (SLC7A11), aldolase A (ALDOA), lysine demethylase 3A (KDM3A), lysine demethylase 5A (KDM5A), Sprouty homolog 2 (SPRY2), lactate dehydrogenase A (LDHA), and phosphoglucomutase 1 (PGM1) (Figure 5B). To further understand HIF1A and hemoglobin gene expression, we immunostained for HIF-1α and hemoglobin-α. A representative image shows staining of HIF-1α in nuclei of young face sites but higher expression was detected in older aged

face sites (Figure 5C and 5D, red arrows). Representative images of hemoglobin-α staining in both arm and face sites highlight an elevated staining intensity throughout the upper granular/stratum corneum layers in arm (Figure 5E) and face (Figure 5F) from older individuals as compared to younger. Interestingly, there was no observable staining increase in the basal layer and through the dermis, further supporting that the presence of hemoglobin-α was epidermally derived and not erythroid.

4 DISCUSSION

The skin is the first line of defense protecting the body from environmental stressors such as solar radiation and pollution. Daily exposure to sunlight is one of the more significant environmental insults that induces DNA damage, oxidative stress, and inflammation in skin. Human skin must maintain robust repair capabilities to prevent cumulative damage triggered by these stressors. However, with age this ability is diminished, and the onset of senescence further hinders the skin's capacity to mitigate stress-induced inflammation and can lead to the presence of chronic low-level inflammation.[18] This phenotype is a key feature of inflammaging. The evidence for the presence of inflammaging in skin has been previously reviewed and it was highlighted that while there are clear signs of an inflammaging microenvironment in skin, further work is needed to better understand it's role on skin aging.[19]

To better understand the role of inflammaging on skin aging, we utilized a systems-biology based approach to investigate biological samples collected from photoprotected and exposed female body sites spanning 6 decades of age. A previous report found that patterns of gene expression accelerated with aging in Caucasian

females and differed in a subgroup that appeared exceptionally youthful based on image analysis of facial appearance.[2] The current study focused on the epidermal skin compartment and employed a systems biology-based approach to increase our understanding and identify potential intervention strategies to mitigate premature aging. Our findings provide a body of evidence that photoexposed facial skin appears to be ~~is~~ in an inflammaging microenvironment due to the presence of elevated chronic inflammation which, in turn, could be a factor in part that leads to an imbalance in epidermal homeostasis starting in the 30's as measured via histology, transcriptomics, and proteomics (Figure 6). This suggests that targeting inflammation in younger aged skin may be a promising intervention approach to mitigate the molecular and morphological changes that lead to a photoaged appearance of skin and impact on underlying skin health.

The histomorphologic analysis in this study found that the epidermis undergoes significant changes with age, including stratum corneum thickening, implying that there may be a stronger barrier in older aged skin. While counter-intuitive, several reported studies have shown that trans-epidermal water loss values decrease in older aged subjects, suggesting that the barrier integrity improves with age.[20] However, the underlying health of the skin plays a role to ensure optimal repair response kinetics to damaging agents. Older aged skin has been shown to have a slower and weaker response profile to damage such as wounding and tape strip removal.[21, 22] We also show that with age the epidermis becomes thinner, the rete ridge path length flattens, and these changes correlate with changes in gene expression and protein levels associated with differentiation and proliferation, similar to *in vitro* data previously

published.[23] Expression changes occur in a large proportion of genes encoding ~~for~~ proteins associated with the epidermal complex, keratins, proteases, protease inhibitors, calcium bindings proteins/AMP, and late cornified envelope proteins. Additionally, these changes are more apparent in the photoexposed arm and face sites than the buttock site, confirming previous *in vitro* data where UVB irradiation led to increased levels of late differentiation markers.[243]~~.~~ This imbalance in differentiation and proliferation processes appears to shift in the 30's and could be a factor in the observed morphological changes detected starting in the 40's. For example, the representative expression traces for FLG, LOR, ALOX12B, KRT2, CALML3, SPINK5, and CSTB all show a similar pattern of increased expression beginning in the 20's to 30's and continuing to increase across the decades. It is worth noting that some of these markers show ~~-~~alterations of this trend in the 50's, presumably due in part to hormonal changes as recorded in the previous study.[2] This is particularly highlighted in the respective traces presented as well as the overall expression patterns for the late cornified envelope proteins which showed significant changes in expression between the 20's and 50's but lost significance when comparing between the 20's and 70's. Several of the proteins expressed by these genes were also detected via proteomics profiling between the photoexposed arm of young and old subjects. A similar proteomics profiling has been reported in which the authors used tape strip collection to quantitate the levels of surface proteins associated with differentation.[2~~3~~45] Their findings are similar to the ones presented here with the exception that several proteins showed contrasting reduced levels in photoexposed skin compared to the elevated levels of those same proteins in our study. It should be pointed out that the age comparison

between the 20's and 60's in this work was selected due to reversal of expression levels in the older 70's cohort. Future work will include additional analyses across all the age groups. Overall, there is an apparent correlation between the differentiation associated gene expression changes that begins in the 20's and correlates with the morphological changes that become significantly measurable starting in the 40's. This suggests an imbalance in epidermal homeostasis which could impact its response profile to environmental insults and maintenance of normal cellular function.

To better understand the inflammatory and photoexposure status of the subjects in this study, we evaluated for the presence of inflammatory and photosensitive biomarkers isolated from the skin's surface. Detection of elevated levels of IL-8 has been shown to be elevated in eczema, atopic dermatitis, and psoriasis skin and in 3D skin models after UVB exposure.[23,6-28] We found elevated levels of IL-8 on photoexposed facial skin surface sites that remain elevated across age groups. The ratio of IL-1RA/IL-1α present on the skin's surface is known to be an indicator of underlying inflammation associated with skin dermatitis conditions and UV exposure.[28,9-30,1] Relative to impact of age and photoexposure on this inflammatory biomarker, it was reported that the IL-1RA/IL-1α ratio was elevated in photoexposed face compared to non-exposed upper inner arm and remained constant across age groups.[28,9] Relatedly, we show similar patterns when comparing between photoexposed face where the IL-RA/IL-lα ratio was consistently high and consistently low in photoprotected buttock sitess across the decades. Surprisingly, we did not see an increase in these cytokines in photoexposed dorsal arm samples since we had previously reported there are significant histological indications of photoaging.[2] We show that several biomarkers

associated with photoexposure are increased in arm sites, including the *cis/trans*-urocanic acid ratio, foci of the DNA damage response marker 53BP1 that is sensitive to UV exposure, and epigenetic age derived from methylation levels of DNA, an indicator of epigenetic aging.[11,3,12-3,34] These methylation patterns are similar to what has been previously reported where the biopsies were enzymatically separated into epidermis and dermis fractions in contrast to LCM in our study.[3,45] Overall, this supports that the photoexposed arms undergo photodamage. We do not believe the lower levels of IL-8 or the IL-1RA/IL-1α ratio on photoexposed arm or buttock sites are an artefact since we performed the analysis in two independent experiments from duplicate tapes. The difference could reflect a dose response or a level of chronic exposure or, alternatively, facial skin is among the thinnest in the body and may be more susceptible to injury. While overall our results support the hypothesis that photoexposed skin is in a heightened state of inflammation, and that inflammation is present early in the 20's and remains persistent across the decades, future work is needed to understand the physiological relevance in photodamaged arms. Overall, the implications of this constant inflammatory pressure could be an indicator of skin inflammaging that leads to the changes in gene expression patterns and correlating protein levels in photoexposed skin.

We previously reported CDKN2A, a gene that encodes for proteins associated with senescence induction, to be elevated with age.[2] CDKN2A is known to encode for $p14^{ARF}$, $p15^{INK4B}$, and $p16^{INK4A}$, all of which are involved in senescence and play significant roles in cancer, and aging, including in skin.[15-17] In the current study we wished to better understand this correlation beyond CDKN2A and performed a focused

transcriptomics profiling of select genes encoding for proteins associated with regulation or induction of senescence in skin.[3,5,6] It has been established that photoexposure can cause keratinocytes to prematurely enter senescence and these cells can be characterized by secretion of an altered secretome called the senescence-associated secretory phenotype (SASP), and is enriched with pro-inflammatory cytokines such as IL-6, IL-8, and IL-1β.[8,]

The elevated skin surface levels of IL-8 early in the 20's age cohort on photoexposed face sites supports there may be an early onset of a SASP--associated phenotype in photodamaged facial skin. We see significant elevated levels of expression of genes encoding for proteins associated with senescence in the photoexposed sites. For example, GLB1 encodes for SA-β-gal (beta-galactosidase), a well-known biomarker of senescence in numerous tissues, including skin.[3,5,6] Several chemokine receptors were observed to increase in expression levels with age in the photoexposed arm and face sites. CXCR1 and CXCR2 encode for receptor proteins that bind with IL-8 and showed elevated expression in both arm and face.[3,6,7] Interestingly this provides a potential correlation of inflammatory response with the elevated levels of IL-8 present on the skin's surface. A survey of candidate SASP components from a comparison between *in vitro* senescence models and *in vivo* tissue and fluid samples showed the elevated presence of CCL22, IL15, and MMP9 under senescent-impacted conditions.[3,7,8] The mammalian target of rapamycin (mTOR) is suggested to be a master regulator of metabolite sensing that impacts senescence induction and overall cellular aging.[3,8,9, 40,39] We show in both photoexposed epidermal sites an increase in mTOR expression levels with age (Figure 4A) that becomes

significant in the 50's compared to the 20's for face (Figure 4B). CREG (cellular repressor of E1A-stimulated genes 1) co-expression with $p16^{INK4a}$ can further enhance senescence than either expressed alone.[401] Recently, CRYAB and HMOX1 have been proposed to be senolytic targets in humans cell models.[412] Interestingly, it was also demonstrated that HMOX1 expression levels were increased during differentiation, which supports a similar correlation as measured in our study.[43232] As reported here, we observe a significant increase in the expression patterns of these genes starting in the 30's and continuing into the 70's in photoexposed facial epidermis sites. In addition, we evaluated genes that encode ~~for~~ proteins that mitigate senescence, including RBL2, SIRT1, SIRT3, SIR4, and TP53.[12,43434–45656] These show varying patterns of decreased expression in the epidermis of photoexposed sites with significance starting in the 50's and 60's. Finally, we immunostained for $p16^{INK4A}$ and detected nuclear localized puncti in both basal and spinous~~al~~ layers. Interestingly, it has been reported that $p16^{INK4a}$ is primarily detected in epidermal melanocytes by immunohistochemistry methods.[46767] However, this may not be an exclusive scenario since it has also been reported that $p16^{INK4a}$ can be detected in keratinocytes in both basal and suprabasal layers, findings that are similar to ours.[48787] These findings suggest that future work is needed to better define the role of this important senescence marker in the skin individual cell types.

In total, the data presented here supports that photoexposed skin is undergoing an accumulation of senescent cells with age. The chronic presence of the SASP factor IL-8 could be a causative indicator of senescence but further work is needed to establish cause and effect linked to the imbalance in differentiation-/proliferation and morphological changes.[46798] The implications of skin undergoing these changes in

inflammation and senescence due to photoexposure also has potential implications on overall body health. A recent review suggests there is a correlation between the accumulation of senescent cells in the skin and a negative impact on overall systemic health and longevity that occurs via the hypothalamic-pituitary-adrenal axis.[4507~~89~~] Future work is planned to further correlate the gene expression and protein detection across individuals and body sites in this data set and from a recent clinical study.

Oxygenation of the epidermis occurs via passive diffusion from direct contact with atmospheric oxygen and from microcapillary beds intertwined underneath the basement membrane.[48~~519~~] This may explain why the epidermis is considered to have a relatively low oxygen tension ~~that has been~~ estimated to range between 0.3-8%, and why the epidermis could be considered hypoxic in contrast to the highly vascularized dermis where oxygen levels are estimated to be >7%.[4501,52~~19~~,50] The morphological changes ~~that were~~ measured in the epidermis with age suggested to us ~~there could be~~ a further limitation of oxygen supply due to the longer diffusion path length through the thickened stratum corneum, as well as the reduced surface area interface with microcapillary beds from reduction of rete ridge undulation pattern. It has been previously reported that aging can lead to a measured increase in hypoxic-related response profiles.[5~~3~~21] That work utilized suction fluid blisters from young and older aged upper arms for transcriptomics profiling. In our study, we utilized the sensitivity of LCM dissection to localize the epidermis in both photoprotected and photoexposed skin sites for further investigation and an overall systems-biology body of evidence. The impact of a lowered oxygen tension in the epidermis is controlled in large part by hypoxia-inducible factor-1α (HIF-1α), a transcription factor and master regulator of cellular

response to oxygen tension condition.[54] In addition to HIF-1~~A~~α, an expanded transcriptomics profiling of select genes encoding proteins associated with regulation or responsiveness to oxygen tension changes or hypoxia supports our hypothesis that photoaged skin is transitioning into a more hypoxic microenvironment. For example, hypoxic conditions have been shown to induce HMOX1 gene expression at 1% O_2 *in vitro* and 7% O_2 *in vivo* and this was mediated by HIF-1α activity.[52345] Gene expression of the CXCL16-CXCR6 axis, CXCR4, and CXCL12 have been reported to be elevated under chronic hypoxic conditions.[56543] PDSS1 encodes for decaprenyl diphosphate synthase subunit 1 and was recently identified as a member of a hypoxia signature in hepatocellular carcinoma cells.[57654] We identified several genes whose expression patterns are negatively regulated under hypoxic conditions. Lysine demethylase 3A (KDM3A) has been reported to regulate PGC1α (PPARGC1A) and is inhibited under hypoxic conditions.[55678] Silencing of SPRY2 gene expression was shown to correlate with elevated levels of HIF-1α.[56789] Prolonged exposure to hypoxic conditions is known to shift cellular metabolism to a greater reliance on glycolysis due to the more anaerobic conditions.[560987] We observed a similar shift based on elevated expression of genes encoding ~~for~~ enzymes involved in glycolysis such as ALDOA, ENO1, LDHA, PGM1, and PKM. This was further supported by the detection of higher protein levels for ADLOA and PKM in older aged arm samples compared to younger aged samples. Expression for the glucose transporters SLC2A1, SLC2A3, and SLC7A11 were also elevated with age, which have been reported to be stimulated in response to hypoxia.[5456,610589] Interestingly, we detected elevated expression of hemoglobin-α and -β (HBA and HBB) and a numerically greater level of hemoglobin-α protein ~~levels~~ in

older aged photoexposed arms. Of note, we did not see any significant staining for hemoglobin-α through the dermis and neither did we identify hemoglobin differences from proteomics of dermal sections (data not shown). While hemoglobin is well known for its role in O_2 and CO_2 gas exchange in red blood cells, an increasing number of non-erythroid tissues have been reported to endogenously express hemoglobin.[62,109] The exact function of hemoglobin in non-erythroid tissue is not clear but it has been speculated it could include regulation of heme, iron and oxygen levels.[63,210] It has also been proposed that hemoglobin plays a role in response to oxidative stress by helping protect against ROS damage.[61,24] Overall, the significant increase in expression of genes associated with hypoxia and glycolytic enzymes suggests a phenotype reflecting a hypoxic microenvironment in photoexposed skin and, to a weaker extent, in non-exposed skin. The reported range of O_2 tension in the epidermis has a broad range between 0.3-8%[50,52,19, 50], and we would propose that in this study cohort the tension was significantly lower in the older age group compared with the younger group. Further work is needed to validate these findings with quantitation of differences in oxygen content in the epidermal compartment as a function of age and photoexposure.

Limitations exist in this study since it is not clear on the causal relationship between the molecular changes ascribed and the cascade across the decades to the morphological changes.

5 CONCLUSIONS

In summary, this systems biology-based approach to analyse inflammatory and photosensitive biomarkers, proteomics, transcriptomics, and immunostaining strongly

suggests that photoexposed facial skin is undergoing inflammaging that begins as early as in the 20's and that multiple biologic pathways are affected in this process. We propose that the chronic presence of inflammation and SASP early in age may contribute to the molecular reprogramming, imbalance of epidermal homeostasis, and morphological changes. The presence of heightened senescence, oxygen sensing/hypoxic response, epigenetic drift, and metabolic shift may also play roles leading to this imbalance. While this work provides further evidence on the role of senescence and inflammation ion~~in~~ impacting ~~skin~~ aging in photoexposed skin, further evidence is still required.[62~~345~~, 63~~456~~] Finally, the detection of non-erythroid-derived hemoglobin in the epidermis is a novel finding that merits further evaluation on its function and role in skin biology and aging.

ACKNOWLEDGEMENTS

We acknowledge the assistance of John C. Bierman in facilitating tape strip analysis.

CONFLICT OF INTEREST

The authors state no conflict of interest. XY, CN, WG, and YCC are full-time employees of Zymo Research Corporation. BBJ, YMD, and JEO are full-time employees of The Procter & Gamble Company.

AUTHOR CONTRIBUTIONS

BBJ, CYRT, CYH, TTL, XY, LC, SP, SB, OD, and JEO conceived the experiments; BBJ, CYRT, CYH, ALS, TTL, XY, CN, WG, YCC, YMD, LC, and PSG performed experiments and analysed the data. JEO wrote the manuscript. All authors reviewed/edited the manuscript.

DATA AVAILABILITY STATEMENT

The data that support the findings of this study are available from the corresponding author upon reasonable request.

ORCID

John E. Oblong https://orcid.org/0000-0001-7628-6242

REFERENCES

1. Yaar M, Gilchrest BA. Photoaging: mechanism, prevention and therapy. *Br J Dermatol*. 2007; **157**:874-887.

2. Kimball AB, Alora-Palli MB, Tamura M, Mullins LA, Soh C, Binder RL, Houston NA, Conley ED, Tung JY, Annunziata NE, Bascom CC, Isfort RJ, Jarrold BB, Kainkaryam R, Rocchetta HL, Swift DD, Tiesman JP, Toyama K, Xu J, Yan X, Osborne R. Age-induced and photoinduced changes in gene expression profiles in facial skin of Caucasian females across 6 decades of age. *J Am Acad Dermatol.* 2018; **78**(1):29-39.

3. Holthöfer H, Virtanen I, Kariniemi AL, Hormia M, Linder E, Miettinen A. Ulex europaeus I lectin as a marker for vascular endothelium in human tissues. *Lab Invest.* 1982; **47**(1): 60-66.

4. Bennett MF, Robinson MK, Baron ED, Cooper KD. Skin immune systems and inflammation: protector of the skin or promoter of aging? *J Inv Derm Symp Proc.* 2008; **13:1**5-19.

5. Zhuang Y, Lyga J. Inflammaging in skin and other tissues – the roles of complement system and macrophage. *Inflamm Allergy Drug Targets.* 2014; **13**:153-161.

6. Kypriotou M, Huber M, Hohl D. The human epidermal differentiation complex: cornified envelope precursors, S100 proteins and the 'fused genes' family. Exp Dermatol. 2012 Sep;21(9):643-9. doi:

7. Rousselle P, Gentilhomme E, Neveux Y. (2017) Markers of Epidermal Proliferation and Differentiation. In: Humbert P, Fanian F, Maibach H, Agache P. (eds) Agache's Measuring the Skin. Springer, Cham. https://doi.org/10.1007/978-3-319-32383-1_37.

8. Fitsiou E, Pulido T, Campisi J, Alimirah F, Demaria M. Cellular senescence and the senescence-associated secretory phenotype as drivers of skin photoaging. *J Invest Dermatol.* 2021; **141**(4S):1119-1126.

9. Shibata A, Jeggo PA. Roles for 53BP1 in the repair of radiation-induced DNA double strand breaks. *DNA Repair (Amst).* 2020; **93**:102915.

10. Lee, J. W., Ratnakumar, K., Hung, K. F., Rokunohe, D., & Kawasumi, M. (2020). Deciphering UV-induced DNA Damage Responses to Prevent and Treat Skin Cancer. *Photochemistry and photobiology*, *96*(3), 478–499.

11. Horvath S. DNA methylation age of human tissues and cell types. *Genome Biol.* 2013; **14**(10):R115.

12. Xu C, Wang L, Fozouni P. *et al.* SIRT1 is downregulated by autophagy in senescence and ageing. *Nat Cell Biol.* 2020; **22**: 1170–1179.

13. Freund A, Laberge RM, Demaria M, Campisi J. Lamin B1 loss is a senescence-associated biomarker. *Mol Biol Cell*. 2012; **23**(11):2066-2075.

14. Dreesen O, Chojnowski A, Ong PF, Zhao TY, Common JE, Lunny D, Lane EB, Lee SJ, Vardy LA, Stewart CL, Colman A. Lamin B1 fluctuations have differential effects on cellular proliferation and senescence. *J Cell Biol.* 2013; **200**(5):605-617.

15. Ressler S, Bartkova J, Niederegger H, Bartek J, Scharffetter-Kochanek K, Jansen-Dürr P, Wlaschek M. $p16^{INK4A}$ is a robust in vivo biomarker of cellular aging in human skin. *Aging Cell.* 2006; **5**(5):379-389.

16. Waaijer ME, Parish WE, Strongitharm BH, van Heemst D, Slagboom PE, de Craen AJ, Sedivy JM, Westendorp RG, Gunn DA, Maier AB. The number of $p16^{INK4a}$ positive cells in human skin reflects biological age. *Aging Cell.* 2012;**11**(4):722-725.

17. LaPak KM, Burd CE. The Molecular Balancing Act of $p16^{INK4a}$ in Cancer and Aging *Mol Cancer Res* 2014; **12**(2):167-183.

18. Ho CY, Dreesen O. Faces of cellular senescence in skin aging. *Mech Ageing Dev.* 2021; **198**:111525.

19. Pilkington SM, Bulfone-Paus S, Griffiths CEM, Watson REB. Inflammaging and the Skin. *J Invest Dermatol.* 2021; **141**(4S):1087-1095.

20. Wilhelm KP, Cua AB, Maibach HI. Skin aging. Effect on transepidermal water loss, stratum corneum hydration, skin surface pH, and casual sebum content. *Arch Dermatol.* 1991; **127**(12):1806-1809.

21. Ghadially R, Brown BE, Sequeira-Martin SM, Feingold KR, Elias PM. The aged epidermal permeability barrier. Structural, functional, and lipid biochemical abnormalities in humans and a senescent murine model. *J Clin Invest.* 1995; **95**(5):2281-2290.

22. Gosain A, DiPietro LA. Aging and wound healing. *World J Surg.* 2004; **28**(3):321-326.

~~22.~~

23. Tan CL, Chin T, Tan CYR, Rovito HA, Quek LS, Oblong JE, Bellanger S. Nicotinamide Metabolism Modulates the Proliferation/Differentiation Balance and Senescence of Human Primary Keratinocytes. *J Invest Dermatol.* 2019; **139**(8):1638-1647.

24. Tan CYR, Tan CL, Chin T, Morenc M, Ho CY, Rovito HA, Quek LS, Soon AL, Lim JSY, Dreesen O, Oblong JE, Bellanger S. Nicotinamide Prevents UVB- and Oxidative Stress–Induced Photoaging in Human Primary Keratinocytes. *J Invest Dermatol*. 2022; **142**(6):1670-1681.

~~23.~~25. Voegeli R, Monneuse JM, Schoop R, Summers B, Rawlings AV. The effect of photodamage on the female Caucasian facial stratum corneum corneome using mass spectrometry-based proteomics. Int *J Cosmet Sci.* 2017; **39**(6):637-652.

~~24.~~26. Sticherling M, Bornscheuer E, Schröder J-M, Christophers E. Localization of NAP-1/IL-8 immunoreactivity in normal and psoriatic skin. *J Invest Dermatol* 1991; **96**: 26-30.

~~25.~~27. Sticherling M, Bornscheuer E, Schröder JM, Christophers E. Immunohistochemical studies on NAP-1/IL-8 in contact eczema and atopic dermatitis. *Arch Dermatol Res* 1992; **284**: 82-85.

~~26.~~28. Amarbayasgalan T, Takahashi H, Dekio I, Morita E. Interleukin-8 content in the stratum corneum as an indicator of the severity of inflammation in the lesions of atopic dermatitis. *Int Arch Allergy Immunol.* 2013; **160**(1):63-74.

~~27.~~29. Hirao T, Aoki H, Yoshida T, Sato Y, Kamoda H. Elevation of interleukin 1 receptor antagonist in the stratum corneum of sun-exposed and ultraviolet B-irradiated human skin. *J Invest Dermatol.* 1996;**106**(5):1102-1107.

~~28.~~30. Terui T, Hirao T, Sato Y, Uesugi T, Honda M, Iguchi M, Matsumura N, Kudoh K, Aiba S, Tagami H. An increased ratio of interleukin-1 receptor antagonist to interleukin-1alpha in inflammatory skin diseases. *Exp Dermatol.* 1998; **7**(6):327-334.

29.31. Perkins MA, Osterhues MA, Farage MA, Robinson MK. A non-invasive method to assess skin irritation and compromised skin conditions using simple tape adsorption of molecular markers of inflammation. *Skin Res Technol.* 2001; **7**(4):227-237.

30.32. de Fine Olivarius F, Wulf HC, Therkildsen P, Poulsen T, Crosby J, Norval M. Urocanic acid isomers: relation to body site, pigmentation, stratum corneum thickness and photosensitivity. *Arch Dermatol Res.* 1997; **289**(9):501-505.

31.33. Uehara F, Miwa S, Tome Y, Hiroshima Y, Yano S, Yamamoto M, Efimova E, Matsumoto Y, Maehara H, Bouvet M, Kanaya F, Hoffman RM. Comparison of UVB and UVC effects on the DNA damage-response protein 53BP1 in human pancreatic cancer. *J Cell Biochem.* 2014; **115**(10):1724-1728.

32.34. Bártová E, Legartová S, Dundr M, Suchánková J. A role of the 53BP1 protein in genome protection: structural and functional characteristics of 53BP1-dependent DNA repair. *Aging (Albany NY)*. 2019; **11**(8):2488-2511.

33.35. Grönniger E, Weber B, Heil O, Peters N, Stäb F, Wenck H, Korn B, Winnefeld M, Lyko F. Aging and chronic sun exposure cause distinct epigenetic changes in human skin. *PLoS Genet.* 2010; **6**(5):e1000971.

34.36. Wang AS, Dreesen O. Biomarkers of Cellular Senescence and Skin Aging. *Front Genet.* 2018; **9**:247.

35.37. Varney ML, Johansson SL, Singh RK. Distinct expression of CXCL8 and its receptors CXCR1 and CXCR2 and their association with vessel density and aggressiveness in malignant melanoma. *Am J Clin Pathol*. 2006; **125**(2):209-216.

36.38. Schafer MJ, Zhang X, Kumar A, Atkinson EJ, Zhu Y, Jachim S, Mazula DL, Brown AK, Berning M, Aversa Z, Kotajarvi B, Bruce CJ, Greason KL, Suri RM, Tracy RP, Cummings SR, White TA, LeBrasseur NK. The senescence-associated secretome as an indicator of age and medical risk. *JCI Insight*. 2020; **5**(12):e133668.

37.39. Xu S, Cai Y, Wei Y. mTOR Signaling from Cellular Senescence to Organismal Aging. *Aging Dis.* 2013; **5**(4):263-273.

38.40. Huang K, Fingar DC. Growing knowledge of the mTOR signaling network. *Semin Cell Dev Biol.* 2014; **36**:79-90.

39.41. Moolmuang B, Tainsky MA. CREG1 enhances $p16^{INK4a}$-induced cellular senescence. *Cell Cycle*. 2011; **10**(3):518-530.

40.42. Limbad C, Doi R, McGirr J, Ciotlos S, Perez K, Clayton ZS, Daya R, Seals DR, Campisi J, Melov S. Senolysis induced by 25-hydroxycholesterol targets CRYAB in multiple cell types. *iScience*. 2022; **25**(2):103848.

41.43. Numata I, Okuyama R, Memezawa A, Ito Y, Takeda K, Furuyama K, Shibahara S, Aiba S. Functional expression of heme oxygenase-1 in human differentiated epidermis and its regulation by cytokines. *J Invest Dermatol.* 2009; **129**(11):2594-2603.

42.44. Alessio N, Bohn W, Rauchberger V, Rizzolio F, Cipollaro M, Rosemann M, Irmler M, Beckers J, Giordano A, Galderisi U. Silencing of RB1 but not of RB2/P130 induces cellular senescence and impairs the differentiation potential of human mesenchymal stem cells. Cell Mol Life Sci. 2013 May;70(9):1637-51.

43.45. Kida Y, Goligorsky MS. Sirtuins, Cell Senescence, and Vascular Aging. *Can J Cardiol.* 2016; **32**(5):634-641.

46. Kim RH, Kang MK, Kim T, Yang P, Bae S, Williams DW, Phung S, Shin KH, Hong C, Park NH. Regulation of p53 during senescence in normal human keratinocytes. *Aging Cell*. 2015; **14**(5):838-846.

47. Victorelli S, Lagnado A, Halim J, Moore W, Talbot D, Barrett K, Chapman J, Birch J, Ogrodnik M, Meves A, Pawlikowski JS, Jurk D, Adams PD, van Heemst D, Beekman M, Slagboom PE, Gunn DA, Passos JF. Senescent human melanocytes drive skin ageing via paracrine telomere dysfunction. *EMBO J.* 2019; **38**(23):e101982.

48. Pavey S, Conroy S, Russell T, Gabrielli B. Ultraviolet radiation induces p16CDKN2A expression in human skin. Cancer Res. 1999 Sep 1;59(17):4185-9

44.49. Demaria M, Desprez PY, Campisi J, Velarde MC. Cell autonomous and non-autonomous effects of senescent cells in the skin. *J Invest Dermatol.* 2015; **135**(7):1722-1726.

45.50. Franco AC, Aveleira C, Cavadas C. Skin senescence: mechanisms and impact on whole-body aging. *Trends Mol Med.* 2022; **28**(2):97-109.

46.51. Stücker M, Struk A, Altmeyer P, Herde M, Baumgärtl H, Lübbers DW. The cutaneous uptake of atmospheric oxygen contributes significantly to the oxygen supply of human dermis and epidermis. *J Physiol.* 2002; **538**:985-994.

47.52. Evans SM, Schrlau AE, Chalian AA, Zhang P, Koch CJ. Oxygen levels in normal and previously irradiated human skin as assessed by EF5 binding. *J Invest Dermatol.* 2006; **126**(12):2596

53. Prahl S, Kueper T, Biernoth T, Wöhrmann Y, Münster A, Fürstenau M, Schmidt M, Schulze C, Wittern KP, Wenck H, Muhr GM, Blatt T. Aging skin is functionally anaerobic: importance of coenzyme Q10 for anti aging skin care. *Biofactors.* 2008; **32**(1-4):245-255.

48.54. Rezvani HR, Ali N, Nissen LJ, Harfouche G, de Verneuil H, Taïeb A, Mazurier F. HIF-1α in epidermis: oxygen sensing, cutaneous angiogenesis, cancer, and non-cancer disorders. *J Invest Dermatol.* 2011; **131**(9):1793-1805.

49.55. Lee PJ, Jiang BH, Chin BY, Iyer NV, Alam J, Semenza GL, Choi AM. Hypoxia-inducible factor-1 mediates transcriptional activation of the heme oxygenase-1 gene in response to hypoxia. *J Biol Chem.* 1997; **272**(9):5375-5381.

50.56. Korbecki J, Kojder K, Kapczuk P, Kupnicka P, Gawrońska-Szklarz B, Gutowska I, Chlubek D, Baranowska-Bosiacka I. The Effect of Hypoxia on the Expression of CXC Chemokines and CXC Chemokine Receptors-A Review of Literature. *Int J Mol Sci.* 2021; **22**(2):843.

51.57. Zhang B, Tang B, Gao J, Li J, Kong L, Qin L. A hypoxia-related signature for clinically predicting diagnosis, prognosis and immune microenvironment of hepatocellular carcinoma patients. *J Transl Med*. 2020; **18**(1):342.

52.58. Qian X, Li X, Shi Z, Bai X, Xia Y, Zheng Y, Xu D, Chen F, You Y, Fang J, Hu Z, Zhou Q, Lu Z. KDM3A Senses Oxygen Availability to Regulate PGC-1α-Mediated Mitochondrial Biogenesis. *Mol Cell.* 2019; **76**(6):885-895.

53.59. Hicks KC, Patel TB. Sprouty2 Protein Regulates Hypoxia-inducible Factor-α (HIFα) Protein Levels and Transcription of HIFα-responsive Genes. *J Biol Chem*. 2016; **291**(32):16787-16801.

54.60. Czyzyk-Krzeska MF. Molecular aspects of oxygen sensing in physiological adaptation to hypoxia. *Respir Physiol*. 1997; **110**(2-3):99-111.

55.61. Airley RE, Mobasheri A. Hypoxic regulation of glucose transport, anaerobic metabolism and angiogenesis in cancer: novel pathways and targets for anticancer therapeutics. *Chemotherapy*. 2007; **53**(4):233-256.

56.62. Saha D, Patgaonkar M, Shroff A, Ayyar K, Bashir T, Reddy KV. Hemoglobin expression in nonerythroid cells: novel or ubiquitous? *Int J Inflam.* 2014; 803237.

57.63. H. Dassen R, Kamps C, Punyadeera F, Dijcks A, de Goeij A, Ederveen G, Dunselman P, Groothuis. Haemoglobin expression in human endometrium, *Human Reproduction*, 2008; **23**(3): 635–641.

58.64. Saha D, Koli S, Reddy KVR. Transcriptional regulation of Hb-α and Hb-β through nuclear factor E2-related factor-2 (Nrf2) activation in human vaginal cells: A novel mechanism of cellular adaptability to oxidative stress. *Am J Reprod Immunol.* 2017; **77**(6).

59.65. Low E, Alimohammadiha G, Smith LA, Costello LF, Przyborski SA, von Zglinicki T, Miwa S. How good is the evidence that cellular senescence causes skin ageing? *Ageing Res Rev*. 2021; **71**:101456.

66. Lee YI, Choi S, Roh WS, Lee JH, Kim TG. Cellular Senescence and Inflammaging in the Skin Microenvironment. *Int J Mol Sci*. 2021; **22**(8):3849.

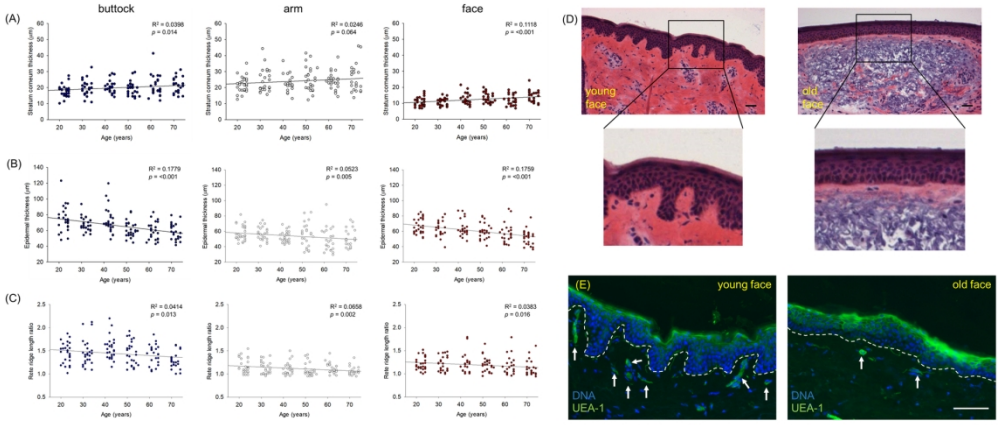

338x190mm (150 x 150 DPI)

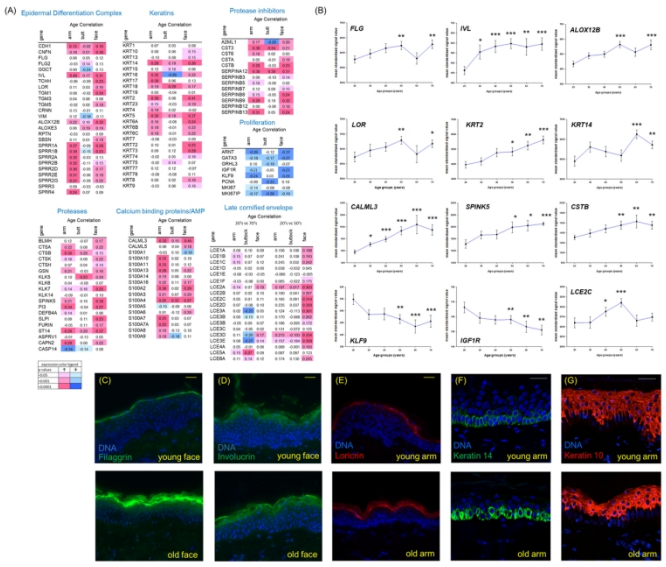

338x190mm (150 x 150 DPI)

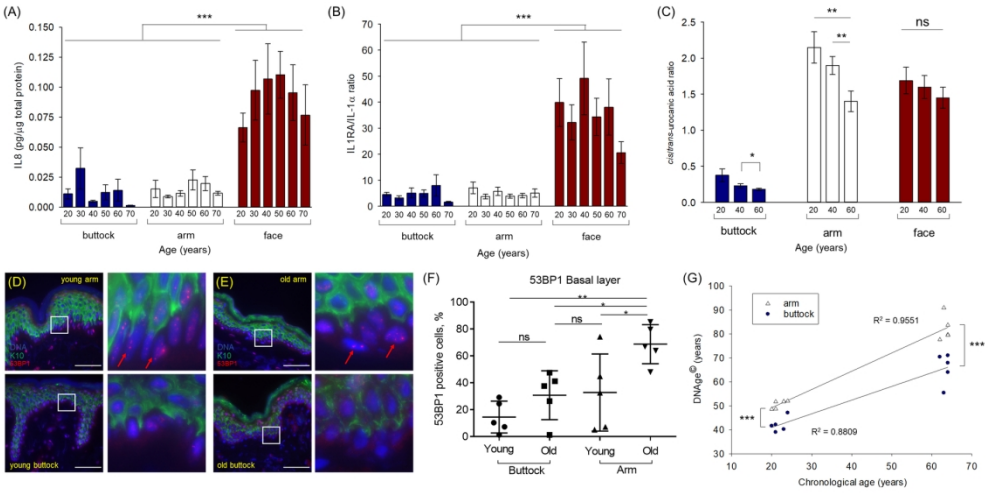

338x190mm (150 x 150 DPI)

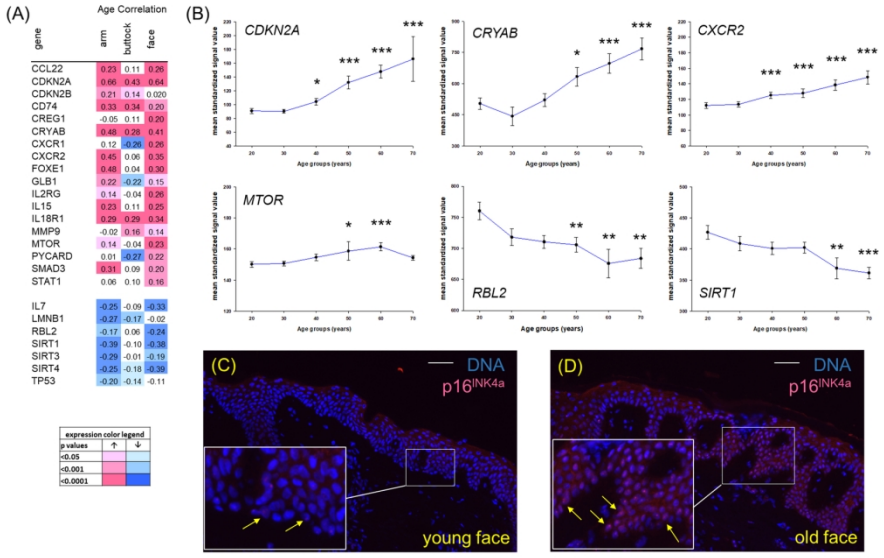

338x190mm (150 x 150 DPI)

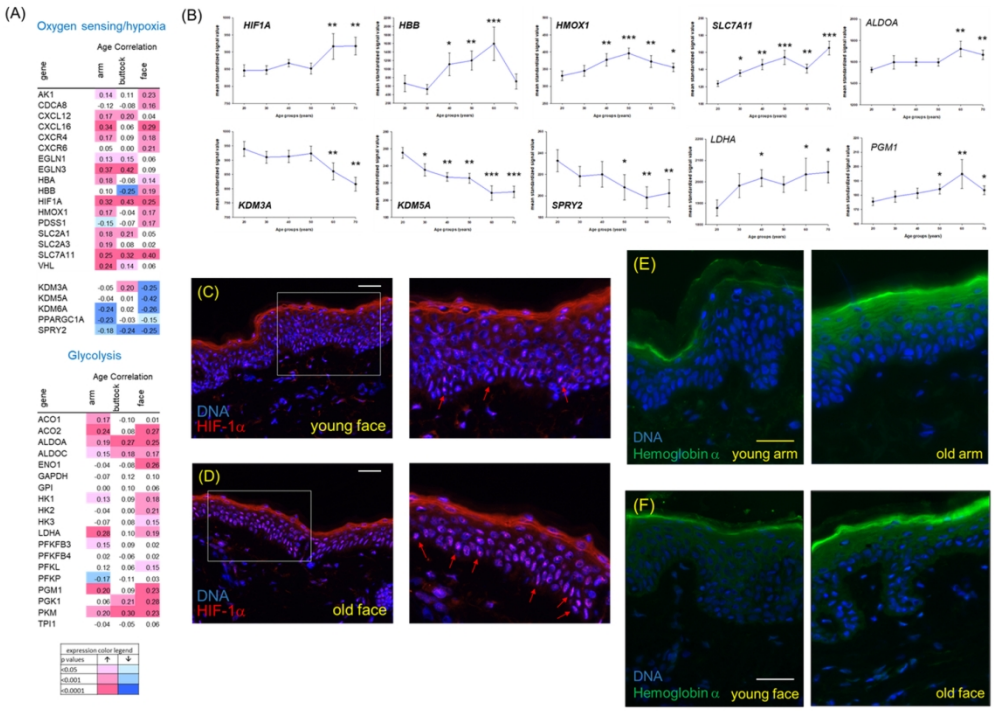

254x190mm (150 x 150 DPI)

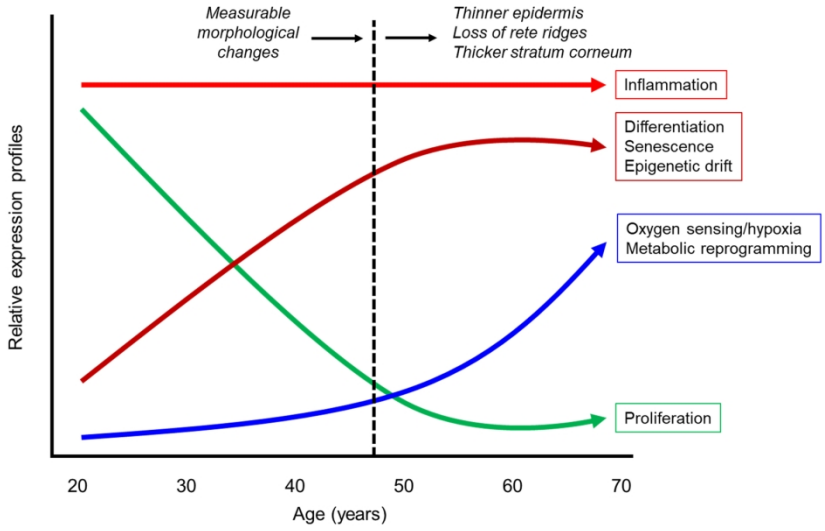

338x190mm (150 x 150 DPI)

Table 2. Median fold change of detected proteins between 60's and 20's age groups from laser capture microdissection sections of epidermis from photoexposed dorsal forearms and changes in gene expression correlation.

Protein	Gene	Median fold change 60's vs 20's	*p*-value	Gene expression changes with age
Keratin 2	KRT2	1.57	<0.001	Increased
Keratin 10	KRT10	1.50	<0.001	Increased
Cystatin M	CST6	1.86	0.001	Increased
Cystatin A	CSTA	2.37	0.002	Increased
Calpain 1	CAPN1	2.33	0.009	No
Fructose-bisphosphate aldolase A	ALDOA	2.04	0.010	Increased
Arachidonate 12 lipoyxgenase 12R	ALOX12B	2.42	0.011	Increased
Bleomycin hydrolase	BLMH	1.73	0.016	Increased
Annexin A8	ANXA8	1.86	0.020	Increased
Cystatin B	CSTB	2.14	0.022	Increased
Annexin A1	ANXA1	1.41	0.026	Increased
Involucrin	IVL	1.47	0.026	Increased
Transglutaminase 1	TGM1	1.38	0.026	Increased
Annexin A2	ANXA2	1.22	0.026	Decreased
Suprabasin	SBSN	1.37	0.026	Increased
Serine protease inhibitor Kazal-type 5	SPINK5	1.43	0.028	Increased
Calmodulin-like protein	CALML3	1.71	0.030	Increased
Malate dehydrogenase 2	MDH2	0.56	0.044	Decreased
Protein S100-A14	S100A14	1.35	0.046	Increased
Pyruvate kinase M	PKM	1.23	0.049	Increased
Gelsolin	GSN	1.23	0.062	Increased
Transglutaminase 3	TGM3	1.45	0.084	Increased
Hemoglobin alpha	HBA	16.40	0.092	Increased

Table 1. Quantification of histological measurements of epidermal morphology across age groups and face, arm, and buttock sites (mean ± SEM).

Body site	Age group	Replicates	Stratum corneum thickness (μm) ± SEM	Epidermal thickness (μm) ± SEM	Rete ridge length ratio ± SEM
Face	20's	30	10.69 ± 0.52	66.67 ± 1.80	1.220 ± 0.025
	30's	24	10.82 ± 0.47	63.25 ± 2.12	1.210 ± 0.032
	40's	24	13.35 ± 0.84*	64.95 ± 2.25	1.242 ± 0.047
	50's	26	13.31 ± 0.63**	60.18 ± 1.88*	1.205 ± 0.030
	60's	22	13.45 ± 1.04*	56.95 ± 2.71**	1.172 ± 0.043
	70's	26	14.44 ± 0.71***	51.92 ± 1.83***	1.086 ± 0.025**
Arm	20's	29	21.98 ± 0.90	57.45 ± 1.76	1.182 ± 0.029
	30's	25	24.30 ± 1.52	56.80 ± 1.70	1.125 ± 0.027
	40's	24	22.94 ± 1.14	52.84 ± 1.48	1.119 ± 0.027
	50's	26	25.45 ± 1.50	55.41 ± 2.86	1.091 ± 0.027*
	60's	22	24.17 ± 1.20	46.25 ± 2.50*	1.098 ± 0.018
	70's	23	25.74 ± 1.94	50.87 ± 2.31*	1.057 ± 0.019*
Buttock	20's	27	17.83 ± 0.69	74.13 ± 2.99	1.449 ± 0.042
	30's	25	19.97 ± 0.97	67.86 ± 1.76	1.464 ± 0.057
	40's	24	20.46 ± 0.78*	72.70 ± 3.33	1.559 ± 0.049
	50's	26	19.10 ± 0.87	61.01 ± 2.04***	1.446 ± 0.049
	60's	22	21.32 ± 1.31*	59.91 ± 2.35***	1.398 ± 0.049
	70's	25	21.23 ± 0.94**	58.91 ± 2.07***	1.300 ± 0.036*

T-test (two tailed, type III) comparing each decade to the 20's age group. * $p<0.05$; ** $p<0.01$; *** $p<0.001$

Table 1. Complete list of detected peptides and corresponding protein associations

Accession	Peptide co	Peptides u	Confidence score	Anova (p)*	Max fold change
K22E_HUMAN	45	45	4001.18	4.66E-06	1.571500921
CDSN_HUMAN	2	2	123.64	5.27E-06	2.437636752
FBX50_HUMAN	1	1	99.35	0.000105	2.384244259
K1C10_HUMAN	34	34	3323.76	0.000116	1.495552411
DSC1_HUMAN	9	9	683.6	0.000851	1.476175156
DIAP2_HUMAN	1	1	41.59	0.000857	2.025061104
GGCT_HUMAN	1	1	61.73	0.001017	2.705299714
CYTM_HUMAN	1	1	48.79	0.001399	1.856927208
PSA6_HUMAN	1	1	83.04	0.00151	2.643433369
CYTA_HUMAN	2	2	156.08	0.001963	2.371513414
DSG1_HUMAN	10	10	828.71	0.002773	1.477494903
RAB7A_HUMAN	2	2	85.13	0.003734	1.770926128
ANK1_HUMAN	1	1	68.47	0.00519	7.557364298
CAN1_HUMAN	2	2	114.65	0.005193	2.333631983
NDKB_HUMAN	1	1	56.79	0.005935	1.837079094
NUCL_HUMAN	3	3	205.82	0.00666	1.49590298
IF6_HUMAN	1	1	73.04	0.007094	1.653846949
H2A2C_HUMAN	2	2	207.97	0.007106	1.332102285
LX12B_HUMAN	1	1	69.59	0.009147	2.423628406
MYL6_HUMAN	3	3	178.28	0.00949	1.316656974
CO6A5_HUMAN	1	1	70.83	0.009747	6.456860767
ALDOA_HUMAN	1	1	54.54	0.010391	2.036634313
ZA2G_HUMAN	1	1	48.27	0.010531	2.029936331
ALBU_HUMAN	19	19	1349.61	0.010736	2.881081964
BLMH_HUMAN	3	3	194.16	0.011627	1.733939166
ANXA8_HUMAN	1	1	42.09	0.011642	1.862656966
FLNA_HUMAN	3	3	226.85	0.012488	1.554708113
RS7_HUMAN	2	2	95.85	0.012869	1.300558293
CYTB_HUMAN	1	1	80.54	0.015614	2.138091331
NDUA4_HUMAN	1	1	72.32	0.016	2.227086503
RAB8B_HUMAN	2	2	115.13	0.017068	1.336733826
EF1A1_HUMAN	3	3	226.36	0.017466	1.282870222
PSA_HUMAN	3	3	137.4	0.019021	2.349263182
ANXA1_HUMAN	3	3	219.29	0.020607	1.406311084
PRDX2_HUMAN	4	4	256.27	0.021337	2.050612602
INVO_HUMAN	3	3	205.86	0.022392	1.471928961
APOA1_HUMAN	4	4	271.12	0.02327	3.900192311
TGM1_HUMAN	3	3	207.73	0.025583	1.376185378
ANXA2_HUMAN	11	11	893.31	0.025828	1.224048837
SBSN_HUMAN	4	4	352.9	0.026108	1.374677388
APEX1_HUMAN	1	1	67.76	0.026309	26.50211607
GSDMA_HUMAN	2	2	114.03	0.026519	2.955793889
ISK5_HUMAN	1	1	68.35	0.02808	1.421964901
CALL3_HUMAN	2	2	152.74	0.030272	1.712491807
RL26_HUMAN	1	1	54.52	0.030846	1.388515772
ACTB_HUMAN	7	7	571.99	0.031106	1.272944065
RL10_HUMAN	1	1	85.89	0.040476	9.486477871
ST2B1_HUMAN	1	1	79.53	0.041009	1.563733606
MDHM_HUMAN	2	2	148.85	0.044087	1.77475996
PLST_HUMAN	4	4	227.88	0.045466	1.241971486
S10AE_HUMAN	2	2	184.54	0.045589	1.353247377
SPB5_HUMAN	4	4	223.27	0.04696	1.176392671
TSYL4_HUMAN	1	1	45.02	0.048409	2.734850233
KPYM_HUMAN	6	6	449.31	0.04853	1.226948687
APOB_HUMAN	1	1	60.54	0.04968	8.327456823
PDIA3_HUMAN	1	1	96.97	0.053799	1.510159821

RS19_HUMAN	2	2	101.11	0.054433	1.596593804
A1AT_HUMAN	1	1	53.89	0.056654	2.413548177
MDHC_HUMAN	1	1	49.96	0.057092	1.317575635
DYL1_HUMAN	1	1	62.55	0.059068	29.69482053
RL13_HUMAN	2	2	92.42	0.059104	2.807482586
PSD12_HUMAN	1	1	56.77	0.060677	2.618455047
CATA_HUMAN	3	3	243.12	0.060771	1.338620482
GELS_HUMAN	2	2	141.25	0.061643	1.22506259
IF2B1_HUMAN	1	1	46.76	0.062498	1.47173751
ASC_HUMAN	2	2	120.91	0.067938	1.507575873
BAF_HUMAN	1	1	61.43	0.068195	3.34046231
IL37_HUMAN	1	1	64.04	0.072633	1.54265532
HUTH_HUMAN	3	3	215.14	0.078286	1.788710235
SPA12_HUMAN	2	2	92.42	0.078347	2.570924584
EF1B_HUMAN	4	4	329.44	0.078604	1.206072326
TRI29_HUMAN	2	2	143.75	0.080577	1.314804431
IMPA2_HUMAN	1	1	43.08	0.081315	1.798828494
BAIP2_HUMAN	1	1	56.71	0.081585	1.353464905
CO4A_HUMAN	1	1	71.9	0.083158	111.5807498
TGM3_HUMAN	3	3	191.55	0.084276	1.45153138
RS5_HUMAN	1	1	46.63	0.085413	1.48519207
PHB_HUMAN	1	1	47.04	0.089393	8.525942679
FABP5_HUMAN	1	1	49.78	0.090108	2.393392434
PP1G_HUMAN	1	1	44	0.090412	2.02663082
HBA_HUMAN	7	7	487.1	0.091746	16.39571503
TKT_HUMAN	2	2	94.8	0.093311	1.439436051
ANT3_HUMAN	1	1	97.49	0.095281	2.487589244
TCPB_HUMAN	1	1	104.4	0.100647	1.230026799
PHB2_HUMAN	2	2	116.76	0.101996	1.296436532
ALDOC_HUMAN	1	1	66.26	0.103326	4.686196427
VINC_HUMAN	1	1	94.35	0.106482	1.673825495
CPNS2_HUMAN	2	2	124.46	0.1128	1.327251292
CO6A1_HUMAN	4	4	334.91	0.114611	1.292702386
FILA_HUMAN	8	8	484.68	0.116327	1.306635059
PLAK_HUMAN	15	15	973.19	0.117649	1.263084589
AL3A2_HUMAN	3	3	175.94	0.119418	1.289438741
AHNK_HUMAN	46	46	3033.22	0.120581	1.207350693
SRSF2_HUMAN	1	1	53.5	0.122788	1.280589001
RS3A_HUMAN	1	1	117	0.127245	1.743769457
RTN3_HUMAN	1	1	59.43	0.131229	1.423837827
SYG_HUMAN	1	1	46.04	0.132212	1.372196025
HBB_HUMAN	11	11	908.57	0.133894	10.62628821
RL18_HUMAN	2	2	161.76	0.135305	1.28518038
ARGI1_HUMAN	5	5	321.8	0.137072	1.22104138
IDE_HUMAN	2	2	113.67	0.138276	2.315818325
PKHA7_HUMAN	1	1	42.46	0.141425	1.639571281
RS20_HUMAN	1	1	53.86	0.141427	1.479954322
RSSA_HUMAN	3	3	232.07	0.141797	1.274400579
PTMA_HUMAN	1	1	52.42	0.145106	1.754683786
DESP_HUMAN	60	60	4229.04	0.14557	1.187991464
TPM3_HUMAN	2	2	114.86	0.148137	1.151896057
TCPZ_HUMAN	1	1	52.26	0.149621	1.329175145
ENOA_HUMAN	1	1	77.96	0.150274	1.347717422
XRCC6_HUMAN	3	3	144.42	0.153645	1.313905465
TWF1_HUMAN	1	1	72.25	0.157613	1.415457964
YBOX1_HUMAN	1	1	92.5	0.158332	3.037368735
GSTP1_HUMAN	1	1	56.68	0.159429	3.050493728
RLA0_HUMAN	2	2	167.84	0.160261	1.30606878
CAH2_HUMAN	3	3	196.35	0.167382	2.700501416
CX7A2_HUMAN	1	1	67.22	0.170297	1.280140886

GLRX1_HUMAN	1	1	49.22	0.172069	Infinity	
COX2_HUMAN	1	1	42.72	0.172728	1.70002341	
NB5R1_HUMAN	2	2	117.25	0.173395	1.245625167	
HXK1_HUMAN	1	1	119.68	0.175121	1.984113652	
VDAC2_HUMAN	2	2	115.64	0.176411	1.241923667	
RBP56_HUMAN	1	1	54.03	0.179495	1.584702417	
SSBP_HUMAN	1	1	85.52	0.18578	1.274073483	
H14_HUMAN	3	3	158.63	0.185891	1.125933233	
HV305_HUMAN	1	1	93.25	0.187104	2.959087701	
CAP1_HUMAN	2	2	168.1	0.189348	1.203550892	
KCRU_HUMAN	1	1	55.55	0.18935	1.218138689	
HNRPK_HUMAN	4	4	284.25	0.190296	1.260475702	
AN32E_HUMAN	1	1	84.11	0.191228	1.885062464	
CLUS_HUMAN	2	2	149.5	0.19559	2.26811272	
PCBP1_HUMAN	3	3	171.55	0.196839	1.191299659	
PSA7L_HUMAN	1	1	90.64	0.197493	1.814301795	
1A23_HUMAN	2	2	123.23	0.197934	1.553453265	
EF1G_HUMAN	1	1	43.14	0.198539	1.257612848	
AN32A_HUMAN	1	1	46.9	0.201663	1.285134372	
EZRI_HUMAN	2	2	112.29	0.206472	1.278334002	
CAZA1_HUMAN	2	2	143.25	0.206942	1.16956259	
PNISR_HUMAN	1	1	47.69	0.20695	1.392523423	
SPB12_HUMAN	3	3	157.06	0.209682	1.18659943	
RL27_HUMAN	2	2	83.37	0.214295	1.229872401	
S10A9_HUMAN	1	1	82.75	0.219733	1.142990893	
C1QBP_HUMAN	2	2	128.21	0.22273	1.282135352	
RAN_HUMAN	2	2	128.98	0.223752	1.108475545	
SEPT7_HUMAN	1	1	42.93	0.228494	1.410874595	
RS12_HUMAN	1	1	53.4	0.230111	11.31375841	
DYHC1_HUMAN	3	3	155.16	0.230795	1.283415739	
K2C80_HUMAN	2	2	128.72	0.233455	1.367455441	
LYPA1_HUMAN	1	1	65.84	0.235087	1.352953317	
PRDX6_HUMAN	4	4	189.37	0.23619	1.217651228	
RL17_HUMAN	1	1	45.3	0.237747	1.359966302	
RL18A_HUMAN	1	1	71.73	0.238336	1.133522236	
PDIA6_HUMAN	1	1	82.53	0.240904	1.133374764	
PEPL_HUMAN	3	3	240.36	0.241276	1.120846368	
HSP71_HUMAN	10	10	815.01	0.246724	1.084090567	
GRP75_HUMAN	1	1	43.68	0.24908	1.150417665	
POF1B_HUMAN	4	4	249.08	0.250155	1.191514045	
CAH1_HUMAN	3	3	227.38	0.253856	5.905970035	
TALDO_HUMAN	2	2	140.12	0.254077	1.137801926	
PP2BA_HUMAN	1	1	42.11	0.257644	1.210087083	
PROF1_HUMAN	2	2	114	0.25895	1.184669154	
TBB5_HUMAN	6	6	510.74	0.259615	1.182941254	
IF4A1_HUMAN	1	1	55.67	0.259735	1.355402896	
F213A_HUMAN	2	2	107.08	0.260541	1.559088822	
ALDH2_HUMAN	2	2	182.26	0.263561	1.130541128	
AT1A1_HUMAN	1	1	50.07	0.266911	1.221288848	
BLVRB_HUMAN	1	1	106.22	0.2678	3.529759843	
S10AG_HUMAN	1	1	79.29	0.272856	1.329595873	
SRP09_HUMAN	1	1	58.34	0.273009	1.542996598	
CALR_HUMAN	1	1	47.74	0.273772	1.659284637	
DSC3_HUMAN	6	6	421.61	0.274857	1.216322102	
ODO1_HUMAN	1	1	43.51	0.275783	1.252335891	
PKP1_HUMAN	14	14	1188.18	0.2774	1.159124089	
COHA1_HUMAN	1	1	47.78	0.278124	1.308317457	
THIO_HUMAN	1	1	41.77	0.279389	1.18135862	
CNBP1_HUMAN	1	1	79.54	0.283892	1.548883216	
CH60_HUMAN	2	2	117.63	0.285422	1.234044948	

FIBB_HUMAN	2	2	107.02	0.28554	2.013345521
A1AG1_HUMAN	2	2	133.7	0.291477	1.789481581
RL4_HUMAN	2	2	113.75	0.297363	1.12467198
CO6A2_HUMAN	5	5	292.98	0.300391	1.14803213
GPNMB_HUMAN	1	1	42.65	0.30091	1.215935259
GLTP_HUMAN	1	1	64.42	0.30105	2.77338197
UBE2N_HUMAN	1	1	46.34	0.30192	1.270007042
PSB2_HUMAN	1	1	46.09	0.302456	1.143489112
CFAB_HUMAN	1	1	43.28	0.303291	4.649336613
AATM_HUMAN	1	1	66.12	0.303958	1.277161347
EF2_HUMAN	6	6	386.8	0.308532	1.141075852
DX39B_HUMAN	1	1	71.24	0.308946	1.134921299
APRV1_HUMAN	1	1	54.73	0.309467	1.147571007
HMGB1_HUMAN	2	2	103.41	0.320708	1.241403699
PDC6I_HUMAN	1	1	78.85	0.324207	1.13989538
LYPD3_HUMAN	1	1	46.28	0.324997	1.515213311
RPN2_HUMAN	1	1	46.86	0.326828	1.215093832
DMKN_HUMAN	1	1	54.86	0.328008	1.18266632
PSA4_HUMAN	1	1	67.69	0.330272	1.180063508
UBP5_HUMAN	1	1	55.83	0.33114	1.050168375
RL22_HUMAN	1	1	62.17	0.332309	1.168757175
GDIB_HUMAN	3	3	209.87	0.333042	1.091784377
SRSF7_HUMAN	1	1	52.64	0.338408	1.210015854
ARF1_HUMAN	1	1	47.59	0.339327	1.463697928
RL19_HUMAN	1	1	62.11	0.340316	1.048885618
TPPP3_HUMAN	2	2	117.32	0.34114	1.313926265
PNPH_HUMAN	1	1	47.57	0.341178	3.442615329
CO3_HUMAN	5	5	393	0.344808	2.548846218
FRIL_HUMAN	1	1	56.3	0.35065	1.204754965
SPTN2_HUMAN	4	4	278.63	0.357526	1.171423451
PPIA_HUMAN	4	4	236.08	0.364011	1.076113437
CALL5_HUMAN	2	2	176.94	0.364704	1.180961381
G3P_HUMAN	5	5	363.51	0.367017	1.080358425
Pierce_RT_Cal_M	16	16	1248.55	0.37197	1.039735554
RS15A_HUMAN	1	1	53.1	0.372938	1.430406717
RL12_HUMAN	2	2	121.63	0.373246	1.643661228
XP32_HUMAN	1	1	47.3	0.374105	1.162749892
TBA1C_HUMAN	7	7	549.63	0.376602	1.093420351
FILA2_HUMAN	5	5	324.06	0.379565	1.248328678
RS13_HUMAN	1	1	54.76	0.379601	1.198477635
HNRPD_HUMAN	4	4	216.29	0.380268	1.070724192
RHG01_HUMAN	1	1	43.95	0.386846	1.160689887
EVPL_HUMAN	4	4	257.66	0.398449	1.062209899
RL7_HUMAN	2	2	130.39	0.399273	1.097255451
XRCC5_HUMAN	2	2	141.2	0.402253	1.221795472
ATPO_HUMAN	1	1	50.5	0.403134	8.016406261
RL3_HUMAN	1	1	58.03	0.408996	1.750260831
CO3A1_HUMAN	2	2	90.73	0.413647	1.189350871
HNRPC_HUMAN	3	3	179.03	0.413993	1.084442602
LDHA_HUMAN	5	5	396.79	0.418869	1.110463722
H33_HUMAN	2	2	116.48	0.419353	1.073305657
NDUA5_HUMAN	1	1	83.53	0.422837	1.024300482
LAMP1_HUMAN	1	1	49.28	0.425327	1.027003179
LEG3_HUMAN	2	2	91.15	0.427292	1.451284409
CLH1_HUMAN	3	3	219.52	0.437441	1.079944913
ARPC4_HUMAN	1	1	49.86	0.439659	1.06737206
RS10_HUMAN	1	1	59.3	0.440776	1.010534196
PSB1_HUMAN	1	1	72.27	0.441774	1.093018298
IF5A2_HUMAN	1	1	59.89	0.447027	1.145088474
HNRPU_HUMAN	1	1	90.24	0.449074	1.264498758

SERA_HUMAN	7	7	480.38	0.454902	1.186328801
CO6A3_HUMAN	20	20	1407.8	0.459252	1.380081667
DHE3_HUMAN	1	1	86.21	0.461354	1.151317171
HNRPQ_HUMAN	3	3	164.89	0.464631	1.047445948
RS18_HUMAN	1	1	58.62	0.465606	1.524293647
SDC1_HUMAN	1	1	89.45	0.468391	1.757744217
TCPE_HUMAN	2	2	139.74	0.469712	1.094329214
HNRH1_HUMAN	2	2	138.9	0.473903	1.080925322
PGS2_HUMAN	2	2	127.77	0.47447	1.027570585
RS4X_HUMAN	1	1	62.56	0.474477	1.030422766
PRDX5_HUMAN	3	3	204.86	0.476147	1.121437617
HS90A_HUMAN	5	5	336.44	0.476629	1.107210242
CAPZB_HUMAN	2	2	109.67	0.479546	1.343424395
RS24_HUMAN	1	1	42.04	0.484497	1.472477151
TRFE_HUMAN	3	3	202.96	0.491079	1.143902495
TERA_HUMAN	6	6	393.18	0.493779	1.037150248
COF1_HUMAN	3	3	287.13	0.496784	1.057358947
SPTB1_HUMAN	1	1	54.5	0.497228	6.728423348
RL14_HUMAN	1	1	94.31	0.50075	1.482633446
FIBA_HUMAN	2	2	169.23	0.51154	2.471058466
LUM_HUMAN	2	2	134.51	0.513001	1.102271459
PGS1_HUMAN	2	2	118.71	0.518124	1.200125679
H90B4_HUMAN	1	1	64.76	0.520173	1.122411979
PGAM1_HUMAN	2	2	140.45	0.525252	1.059613733
RHG29_HUMAN	1	1	49.4	0.527849	1.538171116
LETM1_HUMAN	1	1	54.65	0.527996	1.096218764
PGRC2_HUMAN	1	1	69.9	0.52947	2.632692241
CPSF5_HUMAN	1	1	56.38	0.531843	1.274259694
POSTN_HUMAN	7	7	673.76	0.533097	1.206153997
FAS_HUMAN	1	1	80.36	0.534278	1.498542794
SFPQ_HUMAN	1	1	48.58	0.536181	1.133196076
RL7A_HUMAN	3	3	235.27	0.536491	1.343350728
RL11_HUMAN	2	2	120.59	0.538751	1.13751557
CLIC1_HUMAN	1	1	58.17	0.539369	1.221312612
RTN4_HUMAN	1	1	75.05	0.539583	1.087122959
KTDAP_HUMAN	1	1	79.69	0.541777	1.040397539
TM109_HUMAN	1	1	76.11	0.557161	1.053886636
RS27A_HUMAN	3	3	172.5	0.557832	1.188312351
CD44_HUMAN	1	1	42.8	0.574031	1.672480604
RLA1_HUMAN	1	1	77.37	0.58129	1.110007836
ANXA5_HUMAN	4	4	258.1	0.582668	1.05682398
ARK72_HUMAN	1	1	71.83	0.586222	1.182684332
A2MG_HUMAN	3	3	188	0.587835	1.492801011
TAGL3_HUMAN	1	1	101.5	0.588951	1.059617778
LDHB_HUMAN	2	2	144.45	0.589375	1.385575197
PRS6A_HUMAN	1	1	43.31	0.59262	2.609997906
S10AB_HUMAN	1	1	55.54	0.594816	1.382428536
MIME_HUMAN	1	1	72.97	0.601039	1.056284351
SPTN1_HUMAN	4	4	234.08	0.601518	1.083910053
RS2_HUMAN	2	2	138.22	0.605639	1.154367492
AT1B3_HUMAN	1	1	60.36	0.612114	1.447123375
FUMH_HUMAN	1	1	73.64	0.612964	1.673588197
IGKC_HUMAN	2	2	173.64	0.614378	1.170745303
ATPA_HUMAN	4	4	260.13	0.615379	1.084847169
PDIA1_HUMAN	3	3	172.04	0.625902	1.072666272
H4_HUMAN	5	5	382.17	0.632117	1.153459991
1433Z_HUMAN	7	7	613.91	0.639398	1.018407224
ACTN4_HUMAN	12	12	833.51	0.640636	1.051573425
PKP3_HUMAN	7	7	400.34	0.643648	1.026607377
GBG12_HUMAN	1	1	67.28	0.651131	1.042494667

TADBP_HUMAN	1	1	73.94	0.654911	1.159240843
ANXA4_HUMAN	1	1	100.02	0.656241	2.132093172
AHNK2_HUMAN	4	4	209.74	0.663021	1.896074703
SPB8_HUMAN	1	1	77.69	0.664015	1.862114174
CASPE_HUMAN	5	5	312.12	0.667619	1.066672327
RS16_HUMAN	1	1	49.83	0.669207	1.134217083
RAB5B_HUMAN	1	1	79.57	0.670765	1.048147206
ATPB_HUMAN	3	3	257.27	0.674279	1.315218766
RSMN_HUMAN	1	1	54.18	0.682878	1.402070267
LAD1_HUMAN	1	1	65.8	0.686342	1.117114693
MYH9_HUMAN	16	16	1204.46	0.688162	1.060566385
ADT2_HUMAN	3	3	166.88	0.692299	1.269739958
RS8_HUMAN	2	2	167.64	0.694811	1.698543162
ITB4_HUMAN	1	1	79.05	0.713515	1.075686639
VDAC1_HUMAN	2	2	120.43	0.713883	2.457938516
ICAL_HUMAN	1	1	48.76	0.719556	1.405147237
RL6_HUMAN	1	1	72.18	0.734843	1.675819153
RS3_HUMAN	4	4	252.88	0.738209	1.216720897
ST134_HUMAN	1	1	42.32	0.747419	1.279377606
RL31_HUMAN	1	1	45.59	0.748818	1.009865951
LOXE3_HUMAN	1	1	89.03	0.754121	1.231475939
SET_HUMAN	3	3	181.5	0.764457	1.058847128
IQGA1_HUMAN	7	7	550.66	0.76842	1.139688856
CO1A2_HUMAN	5	5	401.78	0.776975	1.175546753
CO1A1_HUMAN	10	10	828.67	0.7782	1.030813383
RL27A_HUMAN	2	2	108.64	0.778562	1.235029567
ERP29_HUMAN	1	1	43.59	0.781658	1.049598443
CALX_HUMAN	1	1	87.01	0.784239	1.010863185
TCP4_HUMAN	1	1	54.41	0.78781	1.07951747
ASAH1_HUMAN	1	1	44.42	0.791565	1.089146324
PGK1_HUMAN	3	3	216.76	0.795045	1.018283254
RINI_HUMAN	1	1	91.97	0.800057	1.361518647
CIRBP_HUMAN	2	2	138.62	0.805368	1.068332391
TPIS_HUMAN	1	1	84.39	0.806705	1.100539224
MGST3_HUMAN	1	1	101.42	0.807959	1.046743904
LEG7_HUMAN	4	4	379.07	0.812017	1.027119523
LMNA_HUMAN	10	10	833.04	0.818901	1.30739509
KPRP_HUMAN	2	2	92.36	0.821107	1.065735304
CTND1_HUMAN	1	1	63.71	0.82541	1.6591742
RL9_HUMAN	2	2	104.48	0.826601	1.018057815
GATM_HUMAN	1	1	50.72	0.828192	1.23337988
NIBL1_HUMAN	1	1	57.89	0.830195	1.035731982
B3AT_HUMAN	4	4	292.8	0.830951	1.999778403
RL23A_HUMAN	1	1	94.32	0.831145	1.067544229
GTR1_HUMAN	2	2	121.93	0.832782	1.004225524
THIL_HUMAN	1	1	92.76	0.8381	2.413084837
HSP74_HUMAN	1	1	50.01	0.838302	1.64396316
ARPC3_HUMAN	1	1	65.88	0.85073	1.055755578
RL30_HUMAN	1	1	53.29	0.86025	1.001537136
TCPQ_HUMAN	1	1	95.14	0.862432	1.642452431
A2ML1_HUMAN	1	1	52.46	0.865454	2.310167436
H15_HUMAN	1	1	56.07	0.869234	1.041500991
CO7A1_HUMAN	7	7	558.03	0.873386	1.0791599
KCRB_HUMAN	2	2	130.57	0.874225	1.196037893
IGHG1_HUMAN	1	1	52.23	0.879617	1.043311236
RP1BL_HUMAN	1	1	77.35	0.891714	1.232075708
PFKAL_HUMAN	1	1	100.43	0.892456	1.417079162
NEDD8_HUMAN	1	1	49.69	0.894299	1.049405827
RS6_HUMAN	2	2	88.78	0.899267	1.101960717
CTNA1_HUMAN	1	1	76.93	0.906809	1.279621427

RS25_HUMAN	2	2	134.63	0.913145	1.008719707
RS9_HUMAN	4	4	184.06	0.927807	1.011259691
TEBP_HUMAN	1	1	50.91	0.934986	1.738373391
HNRPM_HUMAN	1	1	54.74	0.943217	1.054421384
HSPB1_HUMAN	3	3	192.06	0.96149	1.17516122
TACD2_HUMAN	1	1	101	0.9632	1.197915549
TAGL2_HUMAN	3	3	272.59	0.965337	1.067319142
RLA2_HUMAN	3	3	244.46	0.966359	1.030936816
OLA1_HUMAN	1	1	66.7	0.974289	1.496231185
ROA2_HUMAN	3	3	225.2	0.982472	1.412894986
PRELP_HUMAN	1	1	62.68	0.987995	1.122688091

Highest mean condition	Lowest mean condition	Description
Age 60	Age 20	Keratin, type II cytoskeletal 2 epidermal OS=Homo sapi
Age 60	Age 20	Corneodesmosin OS=Homo sapiens GN=CDSN PE=1
Age 60	Age 20	F-box only protein 50 OS=Homo sapiens GN=NCCRP1
Age 60	Age 20	Keratin, type I cytoskeletal 10 OS=Homo sapiens GN=K
Age 60	Age 20	Desmocollin-1 OS=Homo sapiens GN=DSC1 PE=1 SV
Age 60	Age 20	Protein diaphanous homolog 2 OS=Homo sapiens GN=
Age 60	Age 20	Gamma-glutamylcyclotransferase OS=Homo sapiens G
Age 60	Age 20	Cystatin-M OS=Homo sapiens GN=CST6 PE=1 SV=1
Age 60	Age 20	Proteasome subunit alpha type-6 OS=Homo sapiens G
Age 60	Age 20	Cystatin-A OS=Homo sapiens GN=CSTA PE=1 SV=1
Age 60	Age 20	Desmoglein-1 OS=Homo sapiens GN=DSG1 PE=1 SV=
Age 60	Age 20	Ras-related protein Rab-7a OS=Homo sapiens GN=RA
Age 60	Age 20	Ankyrin-1 OS=Homo sapiens GN=ANK1 PE=1 SV=3
Age 60	Age 20	Calpain-1 catalytic subunit OS=Homo sapiens GN=CAP
Age 60	Age 20	Nucleoside diphosphate kinase B OS=Homo sapiens G
Age 60	Age 20	Nucleolin OS=Homo sapiens GN=NCL PE=1 SV=3
Age 60	Age 20	Eukaryotic translation initiation factor 6 OS=Homo sapie
Age 20	Age 60	Histone H2A type 2-C OS=Homo sapiens GN=HIST2H2
Age 60	Age 20	Arachidonate 12-lipoxygenase, 12R-type OS=Homo sa
Age 60	Age 20	Myosin light polypeptide 6 OS=Homo sapiens GN=MYL
Age 60	Age 20	Collagen alpha-5(VI) chain OS=Homo sapiens GN=CO
Age 60	Age 20	Fructose-bisphosphate aldolase A OS=Homo sapiens C
Age 60	Age 20	Zinc-alpha-2-glycoprotein OS=Homo sapiens GN=AZG
Age 60	Age 20	Serum albumin OS=Homo sapiens GN=ALB PE=1 SV=
Age 60	Age 20	Bleomycin hydrolase OS=Homo sapiens GN=BLMH PE
Age 60	Age 20	Annexin A8 OS=Homo sapiens GN=ANXA8 PE=1 SV=
Age 60	Age 20	Filamin-A OS=Homo sapiens GN=FLNA PE=1 SV=4
Age 20	Age 60	40S ribosomal protein S7 OS=Homo sapiens GN=RPS7
Age 60	Age 20	Cystatin-B OS=Homo sapiens GN=CSTB PE=1 SV=2
Age 20	Age 60	NADH dehydrogenase [ubiquinone] 1 alpha subcomple
Age 60	Age 20	Ras-related protein Rab-8B OS=Homo sapiens GN=RA
Age 60	Age 20	Elongation factor 1-alpha 1 OS=Homo sapiens GN=EEF
Age 20	Age 60	Puromycin-sensitive aminopeptidase OS=Homo sapien
Age 60	Age 20	Annexin A1 OS=Homo sapiens GN=ANXA1 PE=1 SV=
Age 60	Age 20	Peroxiredoxin-2 OS=Homo sapiens GN=PRDX2 PE=1
Age 60	Age 20	Involucrin OS=Homo sapiens GN=IVL PE=1 SV=2
Age 60	Age 20	Apolipoprotein A-I OS=Homo sapiens GN=APOA1 PE=
Age 60	Age 20	Protein-glutamine gamma-glutamyltransferase K OS=H
Age 60	Age 20	Annexin A2 OS=Homo sapiens GN=ANXA2 PE=1 SV=
Age 60	Age 20	Suprabasin OS=Homo sapiens GN=SBSN PE=2 SV=2
Age 20	Age 60	DNA-(apurinic or apyrimidinic site) lyase OS=Homo sap
Age 60	Age 20	Gasdermin-A OS=Homo sapiens GN=GSDMA PE=1 S
Age 60	Age 20	Serine protease inhibitor Kazal-type 5 OS=Homo sapien
Age 60	Age 20	Calmodulin-like protein 3 OS=Homo sapiens GN=CALM
Age 20	Age 60	60S ribosomal protein L26 OS=Homo sapiens GN=RPL
Age 60	Age 20	Actin, cytoplasmic 1 OS=Homo sapiens GN=ACTB PE=
Age 60	Age 20	60S ribosomal protein L10 OS=Homo sapiens GN=RPL
Age 60	Age 20	Sulfotransferase family cytosolic 2B member 1 OS=Hor
Age 20	Age 60	Malate dehydrogenase, mitochondrial OS=Homo sapien
Age 60	Age 20	Plastin-3 OS=Homo sapiens GN=PLS3 PE=1 SV=4
Age 60	Age 20	Protein S100-A14 OS=Homo sapiens GN=S100A14 PE
Age 60	Age 20	Serpin B5 OS=Homo sapiens GN=SERPINB5 PE=1 SV
Age 60	Age 20	Testis-specific Y-encoded-like protein 4 OS=Homo sapi
Age 60	Age 20	Pyruvate kinase PKM OS=Homo sapiens GN=PKM PE
Age 60	Age 20	Apolipoprotein B-100 OS=Homo sapiens GN=APOB PE
Age 60	Age 20	Protein disulfide-isomerase A3 OS=Homo sapiens GN=

Age 60	Age 20	40S ribosomal protein S19 OS=Homo sapiens GN=RPS
Age 60	Age 20	Alpha-1-antitrypsin OS=Homo sapiens GN=SERPINA1
Age 60	Age 20	Malate dehydrogenase, cytoplasmic OS=Homo sapiens
Age 60	Age 20	Dynein light chain 1, cytoplasmic OS=Homo sapiens GI
Age 60	Age 20	60S ribosomal protein L13 OS=Homo sapiens GN=RPL
Age 60	Age 20	26S proteasome non-ATPase regulatory subunit 12 OS
Age 60	Age 20	Catalase OS=Homo sapiens GN=CAT PE=1 SV=3
Age 60	Age 20	Gelsolin OS=Homo sapiens GN=GSN PE=1 SV=1
Age 20	Age 60	Insulin-like growth factor 2 mRNA-binding protein 1 OS=
Age 20	Age 60	Apoptosis-associated speck-like protein containing a CA
Age 20	Age 60	Barrier-to-autointegration factor OS=Homo sapiens GN=
Age 20	Age 60	Interleukin-37 OS=Homo sapiens GN=IL37 PE=1 SV=1
Age 60	Age 20	Histidine ammonia-lyase OS=Homo sapiens GN=HAL P
Age 60	Age 20	Serpin A12 OS=Homo sapiens GN=SERPINA12 PE=1
Age 60	Age 20	Elongation factor 1-beta OS=Homo sapiens GN=EEF1B
Age 60	Age 20	Tripartite motif-containing protein 29 OS=Homo sapiens
Age 60	Age 20	Inositol monophosphatase 2 OS=Homo sapiens GN=IM
Age 20	Age 60	Brain-specific angiogenesis inhibitor 1-associated prote
Age 60	Age 20	Complement C4-A OS=Homo sapiens GN=C4A PE=1 S
Age 60	Age 20	Protein-glutamine gamma-glutamyltransferase E OS=H
Age 20	Age 60	40S ribosomal protein S5 OS=Homo sapiens GN=RPS5
Age 20	Age 60	Prohibitin OS=Homo sapiens GN=PHB PE=1 SV=1
Age 60	Age 20	Fatty acid-binding protein, epidermal OS=Homo sapiens
Age 60	Age 20	Serine/threonine-protein phosphatase PP1-gamma cata
Age 60	Age 20	Hemoglobin subunit alpha OS=Homo sapiens GN=HBA
Age 60	Age 20	Transketolase OS=Homo sapiens GN=TKT PE=1 SV=3
Age 60	Age 20	Antithrombin-III OS=Homo sapiens GN=SERPINC1 PE
Age 20	Age 60	T-complex protein 1 subunit beta OS=Homo sapiens GI
Age 60	Age 20	Prohibitin-2 OS=Homo sapiens GN=PHB2 PE=1 SV=2
Age 60	Age 20	Fructose-bisphosphate aldolase C OS=Homo sapiens C
Age 60	Age 20	Vinculin OS=Homo sapiens GN=VCL PE=1 SV=4
Age 60	Age 20	Calpain small subunit 2 OS=Homo sapiens GN=CAPNS
Age 60	Age 20	Collagen alpha-1(VI) chain OS=Homo sapiens GN=CO
Age 60	Age 20	Filaggrin OS=Homo sapiens GN=FLG PE=1 SV=3
Age 60	Age 20	Junction plakoglobin OS=Homo sapiens GN=JUP PE=1
Age 20	Age 60	Fatty aldehyde dehydrogenase OS=Homo sapiens GN=
Age 60	Age 20	Neuroblast differentiation-associated protein AHNAK OS
Age 60	Age 20	Serine/arginine-rich splicing factor 2 OS=Homo sapiens
Age 20	Age 60	40S ribosomal protein S3a OS=Homo sapiens GN=RPS
Age 20	Age 60	Reticulon-3 OS=Homo sapiens GN=RTN3 PE=1 SV=2
Age 60	Age 20	Glycine--tRNA ligase OS=Homo sapiens GN=GARS PE
Age 60	Age 20	Hemoglobin subunit beta OS=Homo sapiens GN=HBB
Age 60	Age 20	60S ribosomal protein L18 OS=Homo sapiens GN=RPL
Age 60	Age 20	Arginase-1 OS=Homo sapiens GN=ARG1 PE=1 SV=2
Age 60	Age 20	Insulin-degrading enzyme OS=Homo sapiens GN=IDE
Age 20	Age 60	Pleckstrin homology domain-containing family A membe
Age 60	Age 20	40S ribosomal protein S20 OS=Homo sapiens GN=RPS
Age 60	Age 20	40S ribosomal protein SA OS=Homo sapiens GN=RPS
Age 20	Age 60	Prothymosin alpha OS=Homo sapiens GN=PTMA PE=1
Age 60	Age 20	Desmoplakin OS=Homo sapiens GN=DSP PE=1 SV=3
Age 60	Age 20	Tropomyosin alpha-3 chain OS=Homo sapiens GN=TP
Age 60	Age 20	T-complex protein 1 subunit zeta OS=Homo sapiens GI
Age 60	Age 20	Alpha-enolase OS=Homo sapiens GN=ENO1 PE=1 SV
Age 60	Age 20	X-ray repair cross-complementing protein 6 OS=Homo
Age 20	Age 60	Twinfilin-1 OS=Homo sapiens GN=TWF1 PE=1 SV=3
Age 20	Age 60	Nuclease-sensitive element-binding protein 1 OS=Hom
Age 60	Age 20	Glutathione S-transferase P OS=Homo sapiens GN=GS
Age 60	Age 20	60S acidic ribosomal protein P0 OS=Homo sapiens GN
Age 60	Age 20	Carbonic anhydrase 2 OS=Homo sapiens GN=CA2 PE=
Age 60	Age 20	Cytochrome c oxidase subunit 7A2, mitochondrial OS=H

Age 20	Age 60	Glutaredoxin-1 OS=Homo sapiens GN=GLRX PE=1 SV
Age 60	Age 20	Cytochrome c oxidase subunit 2 OS=Homo sapiens GN
Age 20	Age 60	NADH-cytochrome b5 reductase 1 OS=Homo sapiens (
Age 20	Age 60	Hexokinase-1 OS=Homo sapiens GN=HK1 PE=1 SV=3
Age 20	Age 60	Voltage-dependent anion-selective channel protein 2 O
Age 60	Age 20	TATA-binding protein-associated factor 2N OS=Homo s
Age 20	Age 60	Single-stranded DNA-binding protein, mitochondrial OS
Age 60	Age 20	Histone H1.4 OS=Homo sapiens GN=HIST1H1E PE=1
Age 60	Age 20	Ig heavy chain V-III region BRO OS=Homo sapiens PE
Age 60	Age 20	Adenylyl cyclase-associated protein 1 OS=Homo sapien
Age 60	Age 20	Creatine kinase U-type, mitochondrial OS=Homo sapien
Age 60	Age 20	Heterogeneous nuclear ribonucleoprotein K OS=Homo
Age 20	Age 60	Acidic leucine-rich nuclear phosphoprotein 32 family me
Age 60	Age 20	Clusterin OS=Homo sapiens GN=CLU PE=1 SV=1
Age 60	Age 20	Poly(rC)-binding protein 1 OS=Homo sapiens GN=PCB
Age 60	Age 20	Proteasome subunit alpha type-7-like OS=Homo sapier
Age 20	Age 60	HLA class I histocompatibility antigen, A-23 alpha chain
Age 60	Age 20	Elongation factor 1-gamma OS=Homo sapiens GN=EE
Age 20	Age 60	Acidic leucine-rich nuclear phosphoprotein 32 family me
Age 60	Age 20	Ezrin OS=Homo sapiens GN=EZR PE=1 SV=4
Age 60	Age 20	F-actin-capping protein subunit alpha-1 OS=Homo sapi
Age 60	Age 20	Arginine/serine-rich protein PNISR OS=Homo sapiens (
Age 60	Age 20	Serpin B12 OS=Homo sapiens GN=SERPINB12 PE=1
Age 60	Age 20	60S ribosomal protein L27 OS=Homo sapiens GN=RPL
Age 20	Age 60	Protein S100-A9 OS=Homo sapiens GN=S100A9 PE=1
Age 20	Age 60	Complement component 1 Q subcomponent-binding pr
Age 60	Age 20	GTP-binding nuclear protein Ran OS=Homo sapiens GI
Age 60	Age 20	Septin-7 OS=Homo sapiens GN=SEPT7 PE=1 SV=2
Age 20	Age 60	40S ribosomal protein S12 OS=Homo sapiens GN=RPS
Age 20	Age 60	Cytoplasmic dynein 1 heavy chain 1 OS=Homo sapiens
Age 20	Age 60	Keratin, type II cytoskeletal 80 OS=Homo sapiens GN=
Age 60	Age 20	Acyl-protein thioesterase 1 OS=Homo sapiens GN=LYP
Age 60	Age 20	Peroxiredoxin-6 OS=Homo sapiens GN=PRDX6 PE=1
Age 60	Age 20	60S ribosomal protein L17 OS=Homo sapiens GN=RPL
Age 20	Age 60	60S ribosomal protein L18a OS=Homo sapiens GN=RP
Age 60	Age 20	Protein disulfide-isomerase A6 OS=Homo sapiens GN=
Age 60	Age 20	Periplakin OS=Homo sapiens GN=PPL PE=1 SV=4
Age 60	Age 20	Heat shock 70 kDa protein 1A/1B OS=Homo sapiens G
Age 60	Age 20	Stress-70 protein, mitochondrial OS=Homo sapiens GN
Age 60	Age 20	Protein POF1B OS=Homo sapiens GN=POF1B PE=1 S
Age 60	Age 20	Carbonic anhydrase 1 OS=Homo sapiens GN=CA1 PE
Age 60	Age 20	Transaldolase OS=Homo sapiens GN=TALDO1 PE=1 S
Age 60	Age 20	Serine/threonine-protein phosphatase 2B catalytic subu
Age 20	Age 60	Profilin-1 OS=Homo sapiens GN=PFN1 PE=1 SV=2
Age 20	Age 60	Tubulin beta chain OS=Homo sapiens GN=TUBB PE=1
Age 60	Age 20	Eukaryotic initiation factor 4A-I OS=Homo sapiens GN=
Age 60	Age 20	Redox-regulatory protein FAM213A OS=Homo sapiens
Age 20	Age 60	Aldehyde dehydrogenase, mitochondrial OS=Homo sap
Age 20	Age 60	Sodium/potassium-transporting ATPase subunit alpha-1
Age 60	Age 20	Flavin reductase (NADPH) OS=Homo sapiens GN=BLV
Age 60	Age 20	Protein S100-A16 OS=Homo sapiens GN=S100A16 PE
Age 60	Age 20	Signal recognition particle 9 kDa protein OS=Homo sap
Age 20	Age 60	Calreticulin OS=Homo sapiens GN=CALR PE=1 SV=1
Age 60	Age 20	Desmocollin-3 OS=Homo sapiens GN=DSC3 PE=1 SV
Age 20	Age 60	2-oxoglutarate dehydrogenase, mitochondrial OS=Hom
Age 60	Age 20	Plakophilin-1 OS=Homo sapiens GN=PKP1 PE=1 SV=2
Age 60	Age 20	Collagen alpha-1(XVII) chain OS=Homo sapiens GN=C
Age 60	Age 20	Thioredoxin OS=Homo sapiens GN=TXN PE=1 SV=3
Age 60	Age 20	Beta-catenin-interacting protein 1 OS=Homo sapiens G
Age 60	Age 20	60 kDa heat shock protein, mitochondrial OS=Homo sa

Age 60	Age 20	Fibrinogen beta chain OS=Homo sapiens GN=FGB PE=
Age 60	Age 20	Alpha-1-acid glycoprotein 1 OS=Homo sapiens GN=OR
Age 20	Age 60	60S ribosomal protein L4 OS=Homo sapiens GN=RPL4
Age 60	Age 20	Collagen alpha-2(VI) chain OS=Homo sapiens GN=CO
Age 60	Age 20	Transmembrane glycoprotein NMB OS=Homo sapiens
Age 60	Age 20	Glycolipid transfer protein OS=Homo sapiens GN=GLTI
Age 60	Age 20	Ubiquitin-conjugating enzyme E2 N OS=Homo sapiens
Age 60	Age 20	Proteasome subunit beta type-2 OS=Homo sapiens GN
Age 60	Age 20	Complement factor B OS=Homo sapiens GN=CFB PE=
Age 20	Age 60	Aspartate aminotransferase, mitochondrial OS=Homo s
Age 60	Age 20	Elongation factor 2 OS=Homo sapiens GN=EEF2 PE=1
Age 20	Age 60	Spliceosome RNA helicase DDX39B OS=Homo sapien
Age 60	Age 20	Retroviral-like aspartic protease 1 OS=Homo sapiens G
Age 20	Age 60	High mobility group protein B1 OS=Homo sapiens GN=
Age 60	Age 20	Programmed cell death 6-interacting protein OS=Homo
Age 20	Age 60	Ly6/PLAUR domain-containing protein 3 OS=Homo sap
Age 60	Age 20	Dolichyl-diphosphooligosaccharide--protein glycosyltrar
Age 60	Age 20	Dermokine OS=Homo sapiens GN=DMKN PE=1 SV=3
Age 60	Age 20	Proteasome subunit alpha type-4 OS=Homo sapiens G
Age 60	Age 20	Ubiquitin carboxyl-terminal hydrolase 5 OS=Homo sapi
Age 60	Age 20	60S ribosomal protein L22 OS=Homo sapiens GN=RPL
Age 60	Age 20	Rab GDP dissociation inhibitor beta OS=Homo sapiens
Age 60	Age 20	Serine/arginine-rich splicing factor 7 OS=Homo sapiens
Age 20	Age 60	ADP-ribosylation factor 1 OS=Homo sapiens GN=ARF1
Age 60	Age 20	60S ribosomal protein L19 OS=Homo sapiens GN=RPL
Age 60	Age 20	Tubulin polymerization-promoting protein family membe
Age 60	Age 20	Purine nucleoside phosphorylase OS=Homo sapiens G
Age 60	Age 20	Complement C3 OS=Homo sapiens GN=C3 PE=1 SV=
Age 60	Age 20	Ferritin light chain OS=Homo sapiens GN=FTL PE=1 S
Age 20	Age 60	Spectrin beta chain, non-erythrocytic 2 OS=Homo sapie
Age 60	Age 20	Peptidyl-prolyl cis-trans isomerase A OS=Homo sapiens
Age 20	Age 60	Calmodulin-like protein 5 OS=Homo sapiens GN=CALM
Age 60	Age 20	Glyceraldehyde-3-phosphate dehydrogenase OS=Hom
Age 60	Age 20	Pierce_RT_Cal_Mix
Age 60	Age 20	40S ribosomal protein S15a OS=Homo sapiens GN=RP
Age 20	Age 60	60S ribosomal protein L12 OS=Homo sapiens GN=RPL
Age 60	Age 20	Skin-specific protein 32 OS=Homo sapiens GN=XP32 P
Age 20	Age 60	Tubulin alpha-1C chain OS=Homo sapiens GN=TUBA1
Age 60	Age 20	Filaggrin-2 OS=Homo sapiens GN=FLG2 PE=1 SV=1
Age 60	Age 20	40S ribosomal protein S13 OS=Homo sapiens GN=RPS
Age 60	Age 20	Heterogeneous nuclear ribonucleoprotein D0 OS=Hom
Age 60	Age 20	Rho GTPase-activating protein 1 OS=Homo sapiens GI
Age 20	Age 60	Envoplakin OS=Homo sapiens GN=EVPL PE=1 SV=3
Age 60	Age 20	60S ribosomal protein L7 OS=Homo sapiens GN=RPL7
Age 60	Age 20	X-ray repair cross-complementing protein 5 OS=Homo
Age 20	Age 60	ATP synthase subunit O, mitochondrial OS=Homo sapi
Age 60	Age 20	60S ribosomal protein L3 OS=Homo sapiens GN=RPL3
Age 60	Age 20	Collagen alpha-1(III) chain OS=Homo sapiens GN=COI
Age 60	Age 20	Heterogeneous nuclear ribonucleoproteins C1/C2 OS=H
Age 60	Age 20	L-lactate dehydrogenase A chain OS=Homo sapiens GI
Age 60	Age 20	Histone H3.3 OS=Homo sapiens GN=H3F3A PE=1 SV=
Age 20	Age 60	NADH dehydrogenase [ubiquinone] 1 alpha subcomple
Age 60	Age 20	Lysosome-associated membrane glycoprotein 1 OS=Ho
Age 60	Age 20	Galectin-3 OS=Homo sapiens GN=LGALS3 PE=1 SV=5
Age 60	Age 20	Clathrin heavy chain 1 OS=Homo sapiens GN=CLTC P
Age 20	Age 60	Actin-related protein 2/3 complex subunit 4 OS=Homo s
Age 20	Age 60	40S ribosomal protein S10 OS=Homo sapiens GN=RPS
Age 60	Age 20	Proteasome subunit beta type-1 OS=Homo sapiens GN
Age 60	Age 20	Eukaryotic translation initiation factor 5A-2 OS=Homo s
Age 20	Age 60	Heterogeneous nuclear ribonucleoprotein U OS=Homo

Age 20	Age 60	D-3-phosphoglycerate dehydrogenase OS=Homo sapie
Age 20	Age 60	Collagen alpha-3(VI) chain OS=Homo sapiens GN=CO
Age 20	Age 60	Glutamate dehydrogenase 1, mitochondrial OS=Homo
Age 60	Age 20	Heterogeneous nuclear ribonucleoprotein Q OS=Homo
Age 60	Age 20	40S ribosomal protein S18 OS=Homo sapiens GN=RPS
Age 20	Age 60	Syndecan-1 OS=Homo sapiens GN=SDC1 PE=1 SV=3
Age 20	Age 60	T-complex protein 1 subunit epsilon OS=Homo sapiens
Age 60	Age 20	Heterogeneous nuclear ribonucleoprotein H OS=Homo
Age 60	Age 20	Decorin OS=Homo sapiens GN=DCN PE=1 SV=1
Age 60	Age 20	40S ribosomal protein S4, X isoform OS=Homo sapiens
Age 60	Age 20	Peroxiredoxin-5, mitochondrial OS=Homo sapiens GN=
Age 60	Age 20	Heat shock protein HSP 90-alpha OS=Homo sapiens G
Age 20	Age 60	F-actin-capping protein subunit beta OS=Homo sapiens
Age 20	Age 60	40S ribosomal protein S24 OS=Homo sapiens GN=RPS
Age 60	Age 20	Serotransferrin OS=Homo sapiens GN=TF PE=1 SV=3
Age 60	Age 20	Transitional endoplasmic reticulum ATPase OS=Homo
Age 60	Age 20	Cofilin-1 OS=Homo sapiens GN=CFL1 PE=1 SV=3
Age 60	Age 20	Spectrin beta chain, erythrocytic OS=Homo sapiens GN
Age 20	Age 60	60S ribosomal protein L14 OS=Homo sapiens GN=RPL
Age 20	Age 60	Fibrinogen alpha chain OS=Homo sapiens GN=FGA PE
Age 20	Age 60	Lumican OS=Homo sapiens GN=LUM PE=1 SV=2
Age 20	Age 60	Biglycan OS=Homo sapiens GN=BGN PE=1 SV=2
Age 60	Age 20	Putative heat shock protein HSP 90-beta 4 OS=Homo s
Age 20	Age 60	Phosphoglycerate mutase 1 OS=Homo sapiens GN=PG
Age 20	Age 60	Rho GTPase-activating protein 29 OS=Homo sapiens G
Age 60	Age 20	LETM1 and EF-hand domain-containing protein 1, mito
Age 60	Age 20	Membrane-associated progesterone receptor compone
Age 60	Age 20	Cleavage and polyadenylation specificity factor subunit
Age 20	Age 60	Periostin OS=Homo sapiens GN=POSTN PE=1 SV=2
Age 60	Age 20	Fatty acid synthase OS=Homo sapiens GN=FASN PE=
Age 20	Age 60	Splicing factor, proline- and glutamine-rich OS=Homo s
Age 20	Age 60	60S ribosomal protein L7a OS=Homo sapiens GN=RPL
Age 60	Age 20	60S ribosomal protein L11 OS=Homo sapiens GN=RPL
Age 20	Age 60	Chloride intracellular channel protein 1 OS=Homo sapie
Age 60	Age 20	Reticulon-4 OS=Homo sapiens GN=RTN4 PE=1 SV=2
Age 60	Age 20	Keratinocyte differentiation-associated protein OS=Hom
Age 20	Age 60	Transmembrane protein 109 OS=Homo sapiens GN=TI
Age 20	Age 60	Ubiquitin-40S ribosomal protein S27a OS=Homo sapien
Age 60	Age 20	CD44 antigen OS=Homo sapiens GN=CD44 PE=1 SV=
Age 20	Age 60	60S acidic ribosomal protein P1 OS=Homo sapiens GN
Age 60	Age 20	Annexin A5 OS=Homo sapiens GN=ANXA5 PE=1 SV=
Age 20	Age 60	Aflatoxin B1 aldehyde reductase member 2 OS=Homo
Age 60	Age 20	Alpha-2-macroglobulin OS=Homo sapiens GN=A2M PE
Age 20	Age 60	Transgelin-3 OS=Homo sapiens GN=TAGLN3 PE=1 SV
Age 60	Age 20	L-lactate dehydrogenase B chain OS=Homo sapiens GI
Age 20	Age 60	26S protease regulatory subunit 6A OS=Homo sapiens
Age 20	Age 60	Protein S100-A11 OS=Homo sapiens GN=S100A11 PE
Age 20	Age 60	Mimecan OS=Homo sapiens GN=OGN PE=1 SV=1
Age 20	Age 60	Spectrin alpha chain, non-erythrocytic 1 OS=Homo sap
Age 60	Age 20	40S ribosomal protein S2 OS=Homo sapiens GN=RPS2
Age 20	Age 60	Sodium/potassium-transporting ATPase subunit beta-3
Age 20	Age 60	Fumarate hydratase, mitochondrial OS=Homo sapiens
Age 60	Age 20	Ig kappa chain C region OS=Homo sapiens GN=IGKC
Age 20	Age 60	ATP synthase subunit alpha, mitochondrial OS=Homo s
Age 60	Age 20	Protein disulfide-isomerase OS=Homo sapiens GN=P4H
Age 20	Age 60	Histone H4 OS=Homo sapiens GN=HIST1H4A PE=1 S
Age 60	Age 20	14-3-3 protein zeta/delta OS=Homo sapiens GN=YWHA
Age 60	Age 20	Alpha-actinin-4 OS=Homo sapiens GN=ACTN4 PE=1 S
Age 60	Age 20	Plakophilin-3 OS=Homo sapiens GN=PKP3 PE=1 SV=
Age 20	Age 60	Guanine nucleotide-binding protein G(I)/G(S)/G(O) subu

Age 20	Age 60	TAR DNA-binding protein 43 OS=Homo sapiens GN=T
Age 20	Age 60	Annexin A4 OS=Homo sapiens GN=ANXA4 PE=1 SV=
Age 20	Age 60	Protein AHNAK2 OS=Homo sapiens GN=AHNAK2 PE=
Age 20	Age 60	Serpin B8 OS=Homo sapiens GN=SERPINB8 PE=1 SV
Age 60	Age 20	Caspase-14 OS=Homo sapiens GN=CASP14 PE=1 SV
Age 20	Age 60	40S ribosomal protein S16 OS=Homo sapiens GN=RPS
Age 60	Age 20	Ras-related protein Rab-5B OS=Homo sapiens GN=RA
Age 20	Age 60	ATP synthase subunit beta, mitochondrial OS=Homo sa
Age 60	Age 20	Small nuclear ribonucleoprotein-associated protein N O
Age 20	Age 60	Ladinin-1 OS=Homo sapiens GN=LAD1 PE=1 SV=2
Age 60	Age 20	Myosin-9 OS=Homo sapiens GN=MYH9 PE=1 SV=4
Age 20	Age 60	ADP/ATP translocase 2 OS=Homo sapiens GN=SLC25
Age 20	Age 60	40S ribosomal protein S8 OS=Homo sapiens GN=RPS8
Age 60	Age 20	Integrin beta-4 OS=Homo sapiens GN=ITGB4 PE=1 SV
Age 20	Age 60	Voltage-dependent anion-selective channel protein 1 O
Age 60	Age 20	Calpastatin OS=Homo sapiens GN=CAST PE=1 SV=4
Age 20	Age 60	60S ribosomal protein L6 OS=Homo sapiens GN=RPL6
Age 20	Age 60	40S ribosomal protein S3 OS=Homo sapiens GN=RPS3
Age 60	Age 20	Putative protein FAM10A4 OS=Homo sapiens GN=ST1
Age 20	Age 60	60S ribosomal protein L31 OS=Homo sapiens GN=RPL
Age 60	Age 20	Hydroperoxide isomerase ALOXE3 OS=Homo sapiens
Age 20	Age 60	Protein SET OS=Homo sapiens GN=SET PE=1 SV=3
Age 20	Age 60	Ras GTPase-activating-like protein IQGAP1 OS=Homo
Age 20	Age 60	Collagen alpha-2(I) chain OS=Homo sapiens GN=COL
Age 20	Age 60	Collagen alpha-1(I) chain OS=Homo sapiens GN=COL
Age 20	Age 60	60S ribosomal protein L27a OS=Homo sapiens GN=RP
Age 60	Age 20	Endoplasmic reticulum resident protein 29 OS=Homo s
Age 20	Age 60	Calnexin OS=Homo sapiens GN=CANX PE=1 SV=2
Age 20	Age 60	Activated RNA polymerase II transcriptional coactivator
Age 20	Age 60	Acid ceramidase OS=Homo sapiens GN=ASAH1 PE=1
Age 20	Age 60	Phosphoglycerate kinase 1 OS=Homo sapiens GN=PG
Age 20	Age 60	Ribonuclease inhibitor OS=Homo sapiens GN=RNH1 P
Age 60	Age 20	Cold-inducible RNA-binding protein OS=Homo sapiens
Age 20	Age 60	Triosephosphate isomerase OS=Homo sapiens GN=TP
Age 20	Age 60	Microsomal glutathione S-transferase 3 OS=Homo sapi
Age 20	Age 60	Galectin-7 OS=Homo sapiens GN=LGALS7 PE=1 SV=
Age 20	Age 60	Prelamin-A/C OS=Homo sapiens GN=LMNA PE=1 SV=
Age 20	Age 60	Keratinocyte proline-rich protein OS=Homo sapiens GN
Age 20	Age 60	Catenin delta-1 OS=Homo sapiens GN=CTNND1 PE=1
Age 60	Age 20	60S ribosomal protein L9 OS=Homo sapiens GN=RPL9
Age 20	Age 60	Glycine amidinotransferase, mitochondrial OS=Homo s
Age 60	Age 20	Niban-like protein 1 OS=Homo sapiens GN=FAM129B
Age 60	Age 20	Band 3 anion transport protein OS=Homo sapiens GN=
Age 20	Age 60	60S ribosomal protein L23a OS=Homo sapiens GN=RP
Age 60	Age 20	Solute carrier family 2, facilitated glucose transporter m
Age 20	Age 60	Acetyl-CoA acetyltransferase, mitochondrial OS=Homo
Age 20	Age 60	Heat shock 70 kDa protein 4 OS=Homo sapiens GN=H
Age 60	Age 20	Actin-related protein 2/3 complex subunit 3 OS=Homo s
Age 60	Age 20	60S ribosomal protein L30 OS=Homo sapiens GN=RPL
Age 60	Age 20	T-complex protein 1 subunit theta OS=Homo sapiens G
Age 20	Age 60	Alpha-2-macroglobulin-like protein 1 OS=Homo sapiens
Age 20	Age 60	Histone H1.5 OS=Homo sapiens GN=HIST1H1B PE=1
Age 20	Age 60	Collagen alpha-1(VII) chain OS=Homo sapiens GN=CO
Age 20	Age 60	Creatine kinase B-type OS=Homo sapiens GN=CKB PE
Age 60	Age 20	Ig gamma-1 chain C region OS=Homo sapiens GN=IGH
Age 20	Age 60	Ras-related protein Rap-1b-like protein OS=Homo sapi
Age 20	Age 60	ATP-dependent 6-phosphofructokinase, liver type OS=H
Age 20	Age 60	NEDD8 OS=Homo sapiens GN=NEDD8 PE=1 SV=1
Age 20	Age 60	40S ribosomal protein S6 OS=Homo sapiens GN=RPS6
Age 20	Age 60	Catenin alpha-1 OS=Homo sapiens GN=CTNNA1 PE=

Age 60	Age 20	40S ribosomal protein S25 OS=Homo sapiens GN=RPS
Age 20	Age 60	40S ribosomal protein S9 OS=Homo sapiens GN=RPS9
Age 20	Age 60	Prostaglandin E synthase 3 OS=Homo sapiens GN=PT
Age 20	Age 60	Heterogeneous nuclear ribonucleoprotein M OS=Homo
Age 20	Age 60	Heat shock protein beta-1 OS=Homo sapiens GN=HSP
Age 20	Age 60	Tumor-associated calcium signal transducer 2 OS=Hom
Age 20	Age 60	Transgelin-2 OS=Homo sapiens GN=TAGLN2 PE=1 SV
Age 20	Age 60	60S acidic ribosomal protein P2 OS=Homo sapiens GN
Age 20	Age 60	Obg-like ATPase 1 OS=Homo sapiens GN=OLA1 PE=1
Age 20	Age 60	Heterogeneous nuclear ribonucleoproteins A2/B1 OS=H
Age 20	Age 60	Prolargin OS=Homo sapiens GN=PRELP PE=1 SV=1

iens GN=KRT2 PE=1 SV=2
SV=3
I PE=1 SV=1
KRT10 PE=1 SV=6
'=2
=DIAPH2 PE=1 SV=1
GN=GGCT PE=1 SV=1

N=PSMA6 PE=1 SV=1

=2
AB7A PE=1 SV=1

PN1 PE=1 SV=1
GN=NME2 PE=1 SV=1

ens GN=EIF6 PE=1 SV=1
2AC PE=1 SV=4
piens GN=ALOX12B PE=1 SV=1
_6 PE=1 SV=2
L6A5 PE=1 SV=1
GN=ALDOA PE=1 SV=2
P1 PE=1 SV=2
=2
E=1 SV=1
3

7 PE=1 SV=1

x subunit 4 OS=Homo sapiens GN=NDUFA4 PE=1 SV=1
AB8B PE=1 SV=2
F1A1 PE=1 SV=1
s GN=NPEPPS PE=1 SV=2
2
SV=5

=1 SV=1
lomo sapiens GN=TGM1 PE=1 SV=4
2

piens GN=APEX1 PE=1 SV=2
V=4
ns GN=SPINK5 PE=1 SV=2
ML3 PE=1 SV=2
_26 PE=1 SV=1
=1 SV=1
_10 PE=1 SV=4
mo sapiens GN=SULT2B1 PE=1 SV=2
ns GN=MDH2 PE=1 SV=3

E=1 SV=1
V=2
iens GN=TSPYL4 PE=2 SV=2
=1 SV=4
E=1 SV=2
=PDIA3 PE=1 SV=4

S19 PE=1 SV=2
PE=1 SV=3
s GN=MDH1 PE=1 SV=4
N=DYNLL1 PE=1 SV=1
_13 PE=1 SV=4
S=Homo sapiens GN=PSMD12 PE=1 SV=3

=Homo sapiens GN=IGF2BP1 PE=1 SV=2
ARD OS=Homo sapiens GN=PYCARD PE=1 SV=2
=BANF1 PE=1 SV=1
l
PE=1 SV=1
SV=1
B2 PE=1 SV=3
s GN=TRIM29 PE=1 SV=2
MPA2 PE=1 SV=1
ein 2 OS=Homo sapiens GN=BAIAP2 PE=1 SV=1
SV=2
lomo sapiens GN=TGM3 PE=1 SV=4
5 PE=1 SV=4

s GN=FABP5 PE=1 SV=3
alytic subunit OS=Homo sapiens GN=PPP1CC PE=1 SV=1
A1 PE=1 SV=2
3
=1 SV=1
N=CCT2 PE=1 SV=4

GN=ALDOC PE=1 SV=2

S2 PE=2 SV=2
L6A1 PE=1 SV=3

1 SV=3
=ALDH3A2 PE=1 SV=1
S=Homo sapiens GN=AHNAK PE=1 SV=2
s GN=SRSF2 PE=1 SV=4
S3A PE=1 SV=2

E=1 SV=3
PE=1 SV=2
_18 PE=1 SV=2

PE=1 SV=4
er 7 OS=Homo sapiens GN=PLEKHA7 PE=1 SV=2
S20 PE=1 SV=1
SA PE=1 SV=4
1 SV=2

M3 PE=1 SV=2
N=CCT6A PE=1 SV=3
=2
sapiens GN=XRCC6 PE=1 SV=2

o sapiens GN=YBX1 PE=1 SV=3
STP1 PE=1 SV=2
=RPLP0 PE=1 SV=1
=1 SV=2
Homo sapiens GN=COX7A2 PE=1 SV=1

=2
=MT-CO2 PE=1 SV=1
GN=CYB5R1 PE=1 SV=1
3
S=Homo sapiens GN=VDAC2 PE=1 SV=2
sapiens GN=TAF15 PE=1 SV=1
=Homo sapiens GN=SSBP1 PE=1 SV=1
SV=2
=1 SV=1
ns GN=CAP1 PE=1 SV=5
ns GN=CKMT1A PE=1 SV=1
sapiens GN=HNRNPK PE=1 SV=1
ember E OS=Homo sapiens GN=ANP32E PE=1 SV=1

3P1 PE=1 SV=2
ns GN=PSMA8 PE=1 SV=3
OS=Homo sapiens GN=HLA-A PE=1 SV=1
F1G PE=1 SV=3
ember A OS=Homo sapiens GN=ANP32A PE=1 SV=1

iens GN=CAPZA1 PE=1 SV=3
GN=PNISR PE=1 SV=2
SV=1
27 PE=1 SV=2
1 SV=1
otein, mitochondrial OS=Homo sapiens GN=C1QBP PE=1 SV=1
N=RAN PE=1 SV=3

S12 PE=1 SV=3
s GN=DYNC1H1 PE=1 SV=5
KRT80 PE=1 SV=2
PLA1 PE=1 SV=1
SV=3
17 PE=1 SV=3
PL18A PE=1 SV=2
=PDIA6 PE=1 SV=1

GN=HSPA1A PE=1 SV=5
=HSPA9 PE=1 SV=2
SV=3
=1 SV=2
SV=2
unit alpha isoform OS=Homo sapiens GN=PPP3CA PE=1 SV=1

1 SV=2
=EIF4A1 PE=1 SV=1
GN=FAM213A PE=1 SV=3
piens GN=ALDH2 PE=1 SV=2
1 OS=Homo sapiens GN=ATP1A1 PE=1 SV=1
VRB PE=1 SV=3
=1 SV=1
piens GN=SRP9 PE=1 SV=2

=3
o sapiens GN=OGDH PE=1 SV=3
2
COL17A1 PE=1 SV=3

GN=CTNNBIP1 PE=1 SV=1
piens GN=HSPD1 PE=1 SV=2

=1 SV=2
RM1 PE=1 SV=1
4 PE=1 SV=5
L6A2 PE=1 SV=4
GN=GPNMB PE=1 SV=2
P PE=1 SV=3
GN=UBE2N PE=1 SV=1
N=PSMB2 PE=1 SV=1
=1 SV=2
sapiens GN=GOT2 PE=1 SV=3
1 SV=4
s GN=DDX39B PE=1 SV=1
GN=ASPRV1 PE=1 SV=1
HMGB1 PE=1 SV=3
sapiens GN=PDCD6IP PE=1 SV=1
piens GN=LYPD3 PE=1 SV=2
nsferase subunit 2 OS=Homo sapiens GN=RPN2 PE=1 SV=3

N=PSMA4 PE=1 SV=1
ens GN=USP5 PE=1 SV=2
_22 PE=1 SV=2
s GN=GDI2 PE=1 SV=2
s GN=SRSF7 PE=1 SV=1
1 PE=1 SV=2
_19 PE=1 SV=1
er 3 OS=Homo sapiens GN=TPPP3 PE=1 SV=1
GN=PNP PE=1 SV=2
=2
V=2
ens GN=SPTBN2 PE=1 SV=3
s GN=PPIA PE=1 SV=2
ML5 PE=1 SV=2
o sapiens GN=GAPDH PE=1 SV=3

PS15A PE=1 SV=2
_12 PE=1 SV=1
PE=1 SV=1
IC PE=1 SV=1

S13 PE=1 SV=2
o sapiens GN=HNRNPD PE=1 SV=1
N=ARHGAP1 PE=1 SV=1

7 PE=1 SV=1
sapiens GN=XRCC5 PE=1 SV=3
ens GN=ATP5O PE=1 SV=1
3 PE=1 SV=2
L3A1 PE=1 SV=4
Homo sapiens GN=HNRNPC PE=1 SV=4
N=LDHA PE=1 SV=2
=2
x subunit 5 OS=Homo sapiens GN=NDUFA5 PE=1 SV=3
omo sapiens GN=LAMP1 PE=1 SV=3
5
PE=1 SV=5
sapiens GN=ARPC4 PE=1 SV=3
S10 PE=1 SV=1
N=PSMB1 PE=1 SV=2
sapiens GN=EIF5A2 PE=1 SV=3
sapiens GN=HNRNPU PE=1 SV=6

ens GN=PHGDH PE=1 SV=4
L6A3 PE=1 SV=5
sapiens GN=GLUD1 PE=1 SV=2
sapiens GN=SYNCRIP PE=1 SV=2
S18 PE=1 SV=3
3
GN=CCT5 PE=1 SV=1
sapiens GN=HNRNPH1 PE=1 SV=4

s GN=RPS4X PE=1 SV=2
PRDX5 PE=1 SV=4
GN=HSP90AA1 PE=1 SV=5
s GN=CAPZB PE=1 SV=4
S24 PE=1 SV=1

sapiens GN=VCP PE=1 SV=4

N=SPTB PE=1 SV=5
_14 PE=1 SV=4
E=1 SV=2

sapiens GN=HSP90AB4P PE=5 SV=1
GAM1 PE=1 SV=2
GN=ARHGAP29 PE=1 SV=2
chondrial OS=Homo sapiens GN=LETM1 PE=1 SV=1
nt 2 OS=Homo sapiens GN=PGRMC2 PE=1 SV=1
5 OS=Homo sapiens GN=NUDT21 PE=1 SV=1

=1 SV=3
apiens GN=SFPQ PE=1 SV=2
_7A PE=1 SV=2
_11 PE=1 SV=2
ens GN=CLIC1 PE=1 SV=4

no sapiens GN=KRTDAP PE=1 SV=1
MEM109 PE=1 SV=1
ns GN=RPS27A PE=1 SV=2
=3
N=RPLP1 PE=1 SV=1
2
sapiens GN=AKR7A2 PE=1 SV=3
E=1 SV=3
V=2
N=LDHB PE=1 SV=2
GN=PSMC3 PE=1 SV=3
E=1 SV=2

iens GN=SPTAN1 PE=1 SV=3
2 PE=1 SV=2
OS=Homo sapiens GN=ATP1B3 PE=1 SV=1
GN=FH PE=1 SV=3
PE=1 SV=1
sapiens GN=ATP5A1 PE=1 SV=1
HB PE=1 SV=3
SV=2
AZ PE=1 SV=1
SV=2
1
unit gamma-12 OS=Homo sapiens GN=GNG12 PE=1 SV=3

ARDBP PE=1 SV=1
4
=1 SV=2
/=2
/=2
S16 PE=1 SV=2
AB5B PE=1 SV=1
apiens GN=ATP5B PE=1 SV=3
)S=Homo sapiens GN=SNRPN PE=1 SV=1

5A5 PE=1 SV=7
8 PE=1 SV=2
/=5
)S=Homo sapiens GN=VDAC1 PE=1 SV=2

3 PE=1 SV=3
3 PE=1 SV=2
I3P4 PE=5 SV=1
_31 PE=1 SV=1
GN=ALOXE3 PE=1 SV=1

sapiens GN=IQGAP1 PE=1 SV=1
1A2 PE=1 SV=7
1A1 PE=1 SV=5
PL27A PE=1 SV=2
apiens GN=ERP29 PE=1 SV=4

p15 OS=Homo sapiens GN=SUB1 PE=1 SV=3
SV=5
3K1 PE=1 SV=3
PE=1 SV=2
GN=CIRBP PE=1 SV=1
PI1 PE=1 SV=3
iens GN=MGST3 PE=1 SV=1
2
=1
N=KPRP PE=1 SV=1
1 SV=1
9 PE=1 SV=1
apiens GN=GATM PE=1 SV=1
PE=1 SV=3
=SLC4A1 PE=1 SV=3
PL23A PE=1 SV=1
ember 1 OS=Homo sapiens GN=SLC2A1 PE=1 SV=2
sapiens GN=ACAT1 PE=1 SV=1
ISPA4 PE=1 SV=4
sapiens GN=ARPC3 PE=1 SV=3
_30 PE=1 SV=2
GN=CCT8 PE=1 SV=4
s GN=A2ML1 PE=1 SV=3
SV=3
DL7A1 PE=1 SV=2
E=1 SV=1
HG1 PE=1 SV=1
ens PE=2 SV=1
Homo sapiens GN=PFKL PE=1 SV=6

6 PE=1 SV=1
1 SV=1

S25 PE=1 SV=1
9 PE=1 SV=3
GES3 PE=1 SV=1
sapiens GN=HNRNPM PE=1 SV=3
B1 PE=1 SV=2
no sapiens GN=TACSTD2 PE=1 SV=3
V=3
=RPLP2 PE=1 SV=1
1 SV=2
Homo sapiens GN=HNRNPA2B1 PE=1 SV=2

Supplementary Materials and Methods

S.1 Human clinical sample collection and data availably

Collection of skin biopsies and processing for mRNA extraction, target labeling, processing, and analysis has been previously described.[2] The data reported in this paper have been deposited in the Gene Expression Omnibus (GEO) database, https://www.ncbi.nlm.nih.gov/geo (accession no. GSE112660). No other transcriptomics datasets were generated or analyzed for this manuscript.

S.2 Histology and histomorphometry

Histomorphometry was conducted to observe age-associated skin structural alterations. Hematoxylin and eosin staining was performed on 10 μm cryosections from fresh frozen skin biopsies with the Shandon Rapid-Chrome Frozen Section Staining Kit (Thermofisher Scientific, Kalamazoo, MI) according to manufacturer's recommendations. Sections were fixed with Rapid-Fix, stained with Gill 3 hematoxylin and Eosin-Y, dehydrated with 95% and 100% ethanol, and cleared in xylene. Cover slips were mounted with Shandon Mounting Media (Thermofisher Scientific, Kalamazoo, MI). 10X bright field images of each biopsy were captured with an Olympus BX61 microscope utilizing Cellsens Dimension™ software. Image Pro Premier software (Mediacybernetics, Rockville, MD) was used to measure epidermal thickness, rete ridge path length and stratum corneum thickness in each biopsy. The thickness of the viable epidermal was measured by tracing two separate lines along the dermal epidermal junction (DEJ) and the epidermal granular

layer, then calculating the average distance between these two lines across the entire epidermal length. Rete ridge path length was measured by taking the ratio of the DEJ length to that of the granular layer. Stratum corneum thickness was measured on 20X bright field images by tracing two separate lines along both the epidermal granular layer and the top of the stratum corneum, then calculating the average distance between these two lines across the entire epidermal length.

S.3 Proteomics

For proteomics analysis (n=5 each of 20's and 60's photo-exposed arm samples), epidermal LCM sections were solubilized in 25 μl 0.5M TEAB (triethylammonium bicarbonate) containing 0.1% Rapigest. A 2 μl aliquot is taken for AAA (Amino Acid Analysis), and to the remaining amount 2.5 μl of 50 μM TCEP is added to reduce the cysteine residues. 1.3 μl of 200 μM MMTS was added to block cysteines. The proteins mixture was digested with LysC (1:10 wt/wt ratio) for 4 hours at 37°C, followed by trypsin addition to the mixture for digestion overnight at 37°C. Digest were then acidified and desalted using a micro-spin C18 RP column. Eluted peptide mixture was dried and reconstituted in UPLC loading Buffer A (0.1% formic acid) and Labelfree quantitative LC-MS/MS was performed on an LTQ Orbitrap Elite (ThermoFisher Scientific) equipped with a Waters Symmetry® C18 (180 μm x 20 mm) trap column and a 1.7 μm, 75 μm x 250 mm nanoAcquity™ UPLC™ column (35ºC). Trapping was done using 99% Buffer A (100% water, 0.1% formic acid) and peptide separation was undertaken using a linear gradient of solvents A (0.1% formic acid in water) and B

(0.075% formic acid in acetonitrile) over 210 minutes, at a flow rate of 300 nL/min. MS spectra was acquired in the Orbitrap using 1 microscan and a maximum injection time of 900 ms followed by three data dependant MS/MS acquisitions in the ion trap (with precursor ions threshold of >3000). The total cycle time for both MS and MS/MS acquisition was 2.4 seconds. Peaks targeted for MS/MS fragmentation by collision induced dissociation (CID) were first isolated with a 2 Da window followed by normalized collision energy of 35%. Dynamic exclusion was activated where former target ions were excluded for 30 seconds.

Feature extraction, chromatographic/spectral alignment, data filtering, and statistical analysis were performed using Non-linear Dynamics Progenesis LCMS software (Non-linear Dynamics, LLC). First, the raw data files were imported into the program. A sample run was chosen as a reference (usually at or near the middle of all runs in a set), and all other runs were automatically aligned to that run in order to minimize retention time (RT) variability between runs. No adjustments are necessary in the m/z dimension due to the high mass accuracy of the mass spectrometer (typically <3 ppm). All runs were selected for detection with an automatic detection limit. Features within RT ranges of 0–16 min and 102–120 min was filtered out, as were features with charge ≥ +8. A normalization factor was then calculated for each run to account for differences in sample loading between injections. The experimental design was set up to group multiple injections from each run. The algorithm then calculates and tabulates raw and normalized abundances, max fold change, and ANOVA p-values for each feature in the data set. The MS/MS collected for the experiment were filtered to exclude spectra with rank > 10 or isotope > 3 to ensure that the highest quality MS/MS spectral data are

utilized for peptide assignments and subsequent protein ID. The remaining MS/MS were exported to an .mgf (Mascot generic file) for database searching. After the Mascot search, an .xml file of the results was created, and then imported into the Progenesis LCMS software, where search hits were assigned to corresponding features.

S.4 Skin surface biomarker analysis

Stratum corneum material was collected from each subject's dorsal arm, cheek, and buttock sites. Two sets of three sequential D-Squame tape strip samples (standard sampling discs, 22-mm diameter; CuDerm Corp., Dallas, TX, USA) were collected from each site. Tapes 2 and 3 from an individual site were designated for IL-8 and IL-1RA/IL-1α ratio analysis and tapes 2 and 3 from a neighboring site were used for biochemical metabolite analysis. The tape samples were collected, stored at -80°C, and total protein and metabolites were extracted as previously described.[Kerr] IL-1RA and IL-1α levels were measured by ELISA analysis as per manufacturer's instructions (Bio-Plex Pro Human Cytokine IL-1RA and IL-1α kits, Bio-Rad, Hercules, CA, USA). IL-8 was quantified using Meso Scale Discovery (MSD) electrochemiluminescence V-Plex kit as per manufacturer's instructions and normalized to the amount of soluble total protein as determined by BCA protein assay (BCA™ Protein Assay Kit, Pierce Biotechnology/Thermo Scientific, Rockford, IL, USA). For *cis*- and *trans*-urocanic acid metabolite profiling, individual tubes containing D-Squame strips were pooled to generate 120 samples with 5 replicates per each collection site from 20's, 40's, and 60's age groups. Metabolomic profiling analysis was performed by Metabolon Inc. (Durham,

NC, USA) as previously described.[1] Welch's two-sample *t*-test, matched pair *t*-test, and Principal Component Analysis (PCA) were used to analyze the data.

[1]Evans AM, DeHaven CD, Barrett T, Mitchell M, Milgram E. Integrated, nontargeted ultrahigh performance liquid chromatography/electrospray ionization tandem mass spectrometry platform for the identification and relative quantification of the small-molecule complement of biological systems. *Analytical chemistry* 2009: **81**: 6656–6667.

S.5 Epigenetic Aging clock (DNAge®)

Skin DNA was bisulfite converted using the EZ DNA Methylation-Lightning™ Kit (Zymo Research, Irvine, CA, USA) according to the manufacturer's instructions. Bisulfite-converted DNA libraries contains >2,000 age-associated CpG loci were prepared for Simplified Whole-panel Amplification Reaction Method (SWARM®) platform, which is a targeted bisulfite-based approach where specific CpG loci were sequenced at >1,000x coverage on a HiSeq sequencer. Sequence reads were identified by base calling software then aligned to the hg19 genome using Bismark, an aligner optimized for bisulfited converted sequences. Methylation levels for each cytosine were calculated by dividing the number of reads reporting a "C" by the number of reads reporting a "C" or "T." The methylation level of >2,000 age-associated CpG loci were used for age prediction using Zymo Research's proprietary DNAge® predictor.

S.6 Immunofluorescence and immunohistology

CDKN2A/p16^{INK4a}

7 μm fresh frozen cryosections were fixed in ice cold acetone for 10 minutes at -20°C, washed in phosphate-buffered saline (PBS), and incubated for 1 hour at room temperature (RT) in 10% normal goat serum in PBS (Cell Signaling Tech, Danvers, MA 5425S). Sections were incubated 1 hour at RT with an anti-CDKN2A/p16^{INK4a} (Abcam, Waltham, MA, ab108349 1:500) antibody, washed in PBS, incubated with an Alexa Fluor 555-conjugated goat anti-rabbit antibody (Abcam, Waltham, MA, ab150086 1:1000) for 1 hour at RT, washed in PBS and counterstained with DAPI using NucBlue fixed cell stain Ready Probes reagent (Invitrogen, Carlsbad, CA). Staining of sections minus the primary antibody served as a negative control and displayed no non-specific staining (data not shown). For comparison fluorescent images of young and old biopsies were captured with a Zeiss Observer.Z1 microscope (Carl Zeiss Microimaging, Germany) at equal gamma values, pixel range and exposures.

HIF-1α

7 μm fresh frozen cryosections were fixed in ice cold acetone for 10 minutes at -20°C, washed in PBS, and incubated for 1 hour at RT in 10% normal goat serum in PBS (Cell Signaling Tech, Danvers, MA 5425S). Sections were incubated overnight at 4°C with an anti-HIF-1α antibody (Sigma, ST. Louis, MO, HPA001275 1:100), washed in PBS, incubated with an Alexa Fluor 555-conjugated goat anti-mouse antibody (Abcam, Waltham, MA, ab150118 1:1000) for 1 hour at RT, washed in PBS, and counterstained with DAPI using NucBlue fixed cell stain Ready Probes reagent (Invitrogen Carlsbad, CA). Staining of sections minus the primary antibody severed as a negative control and

displayed no non-specific staining (data not shown). For comparison fluorescent images of young and old biopsies were captured with a Zeiss Observer.Z1 microscope (Carl Zeiss Microimaging, Germany) at equal gamma values, pixel range and exposures.

Hemoglobin-α

7 μm fresh frozen cryosections were fixed in ice cold Acetone for 10 minutes at -20°C, washed in (PBS), and incubated for 30 minutes at RT in 5% normal mouse serum in PBS (Invitrogen Carlsbad, CA, 31881). Sections were incubated 90 minutes at RT with an anti-hemoglobin-α antibody (Santa Cruz Biotech, Dallas, TX, sc-514378 AF488 1:100), washed in PBS, counterstained using NucBlue fixed cell stain Ready Probes reagent (Invitrogen CA, U.S.A.). Mouse IgG1 isotype negative controls (Invitrogen Carlsbad, CA MA5-18167 1:100) displayed no non-specific staining. For comparison fluorescent images of young and old biopsies were captured with a Zeiss Observer.Z1 microscope (Carl Zeiss Microimaging, Germany) at equal gamma values, pixel range and exposures.

Blood vessel staining utilizing *Ulex Europaeus*-I Lectin (UEA-1)

7 μm fresh frozen cryosections were fixed in 95% ethanol at RT for 2 minutes, washed in PBS, and incubated with FITC conjugated UEA-1 (Sigma, St. Louis, MO, L9006 1:50 in water) for 2 minutes at RT, washed in PBS, and coverslipped using Fluorshield with DAPI (Sigma, MO, U.S.A., F6057). For comparison fluorescent images of young and

old biopsies were captured with a Zeiss Observer.Z1 microscope (Carl Zeiss Microimaging, Germany) at equal gamma values, pixel range and exposures.

53BP1

Frozen skin sections were briefly thawed and circled with a hydrophobic barrier pen. Sections were rehydrated with PBS and were fixed with 3% paraformaldehyde for 15 minutes at RT. After 2 washes in PBS, sections were subsequently permeabilized with 0.5% Triton-X for 10 minutes at RT. After 3 washes in PBS, sections were blocked with 5% normal donkey serum for 30 minutes at RT. Subsequently, they were incubated overnight in primary antibodies (1:1000 anti-53BP1 Novus Biologicals and 1:250 anti-K10 Dako in 5% normal donkey serum) at 4°C in a humidified chamber. After 3 washes in PBS, appropriate fluorophore-conjugated secondary antibodies (1:800 donkey anti-rabbit Alexa Fluor 564, 1:800 donkey anti-mouse Alexa Fluor 488 in 5% normal donkey serum) were added for 1 hour at RT. Hoechst dye was used as a nuclear counter-stain. After 3 washes in PBS, sections were mounted in Prolong-Diamond Anti-Fade reagent. Imaging was done at 60X magnification on an Olympus IX-83 inverted fluorescence microscope. Z-stacks were acquired for each position along the length of the skin sample. Projection images were made for each position using Image J and the number of cells showing visible 53BP1 foci were quantified in the K10-positive suprabasal layer and K10-negative basal layer.

Filaggrin and Involucrin

10 μm fresh frozen sections were fixed in ice cold acetone and methanol (1:1) for 10 minutes at -20°C, washed in PBS and incubated for 1 hour at RT in 10% normal goat serum in PBS (Cell Signaling Tech, Danvers, MA 5425S). Sections were incubated overnight at 4°C with an anti-filaggrin (Abcam, Waltham, MA, ab3137 1:100) or an anti-involucrin (Sigma, St. Louis, MO, I9018 1:100) antibody, washed in PBS, incubated with Alexa Fluor 488 conjugated goat anti-mouse antibodies (Abcam, Waltham, MA, ab1500113 1:500) for 1 hour at RT, washed in PBS, and mounted with fluoroshield containing DAPI (Sigma, St. Louis, MO, F6057). Mouse IgG1 isotype negative controls (Invitrogen Carlsbad, CA MA5-18167 1:100) displayed no non-specific staining (data not shown). For comparison fluorescent images of young and old biopsies were captured with a Zeiss Observer.Z1 microscope (Carl Zeiss Microimaging, Germany) at equal gamma values, pixel range and exposures.

Loricrin

7 μm fresh frozen sections were fixed in ice-cold 50% acetone/50% methanol at RT for 5 minutes. Sections were air dried followed by 3 washes in PBS/0.05% Tween 20. They were then blocked with 10% goat serum in PBS for 30 minutes. Subsequently, sections were exposed to anti-loricrin antibody (1:500; Abcam, Singapore, Singapore, ab176322) for 1 hour followed by a 30-minute incubation with an anti-rabbit Alexa Fluor 568 (1:1000; Thermo Fisher, Singapore, Singapore) and a 10-minute counterstain with DAPI (Sigma–Aldrich, Singapore, Singapore) before mounting with Hydromount™ (Electron Microscopy Sciences).

Keratin 14 and Keratin 10

Skin biopsies were fixed in 4% paraformaldehyde (Sigma-Aldrich, Missouri, United States), serially dehydrated in ethanol, then incubated in Histo-Clear (Scientific Laboratory Supplies, Nottingham, United Kingdom) for 30 minutes, and a 1:1 ratio of Histo-Clear and paraffin wax (Thermo Fisher Scientific, Massachusetts, United States) for 60 minutes. Models were incubated in paraffin wax for 1 hour at 65^{o}C prior to embedding (Solmedia Ltd, Shrewsbury, United Kingdom). 5 µm sections were generated using a microtome (Leica, Wetzlar, Germany) and transferred onto charged microscope slides (Thermo Fisher Scientific). Skin sections were deparaffinised in Histo-Clear and rehydrated from 100% ethanol to PBS. Antigen retrieval was performed using pH 6 citrate buffer at 95^{o}C for 20 minutes. Samples were blocked and permeabilised for 1 hour in a blocking buffer of 20% neonatal calf serum (Thermo Fisher Scientific, Massachusetts, United States) in 0.4% Triton X-100 in PBS. Sections were incubated overnight in primary antibodies (1:100 cytokeratin 14 ab7800; 1:100 cytokeratin 10 ab76318; Abcam, Cambridge, UK) at 4^{o}C in a humidified chamber. After 3 washes in PBS, appropriate fluorophore-conjugated secondary antibodies (1:1000 donkey anti-mouse Alexa Fluor® 488, 1:1000 donkey anti-rabbit Alexa Fluor® 594) were added for 1 hour at RT. After 3 washes in PBS, sections were mounted in Vectashield Hardset with DAPI mounting medium (Vector Laboratories, Peterborough, United Kingdom). 40X images were captured at equal gamma values, pixel range and exposures using a Zeiss 880 confocal microscope (Zeiss, Oberkochen, Germany) with Zen software.